Air Flow in Automotive Engines

Authors: Devin Guerrera, William Kelly, Joseph Scafidi, Peter Springer, Erik Wegge

Submitted to: Professor Selçuk Güçeri,

Submitted on: March 25th, 2022

Table of Contents

Table of Figures

Abstract

The purpose of this project was to analyze and optimize the flow of incoming air and outgoing exhaust through an automotive internal combustion engine in order to improve the engine power output in a reliable manner.

The testing vehicle used was a 1997 Chevrolet Corvette that started with the factory V8 engine. The engine build design choices were made through research and analysis with the goal to optimize airflow and support increased component stresses due to the increase in power. Computational fluid dynamics (CFD) was utilized to model fluid flow throughout the intake manifold and further analyze changes that occurred between engine components. Horsepower output measurements were taken before and after modifications to determine power gains and evaluate build design choices.

Acknowledgements

The Air Flow in Automotive Engines team would like to thank several people and groups who were integral to our success and contributed greatly towards our work.

- First, our sincere gratitude to Professor Selçuk Güçeri of WPI's Mechanical Engineering Department. Professor Güçeri advised our project and took his personal time to keep us tight to deadlines, provided supporting information, and always led us on a forward path. All members of the group have enrolled in many of his classes beforehand, and it was special to be able to apply the information he taught to a much more personal project under his mentorship. His efforts, experience, and knowledge of automotive engines and processes was crucial in the group's completion of our work.

- Thank you to the Bowtie Shop in Billerica, Massachusetts who generously provided us a location to work on the project in addition to the numerous tools required for completion. They additionally provided knowledge and mentorship of many of the technicians to help us progress through any setbacks or issues encountered through the duration of our work and this project would not be possible to complete without this space.

- Lastly, thank you to Worcester Polytechnic Institute for funding a significant portion of the project. With the high costs of acquiring many of the components needed for such a technical project, it was relieving for the group to be provided additional financial aid in purchasing many of the necessary components.

Executive Summary

Introduction

Background

The 1997 Chevrolet Corvette

The specific vehicle used for the project was a 1997 C5 Chevrolet Corvette.Chevrolet is a General Motors company (GM) and has been producing the Corvette since 1953. Corvette's are a commonly known "American Muscle" two door luxury sports car that has come in a variety of different options and trim levels as it has developed over the past 70 years. "C5" refers to the specific generation of our Corvette-starting in 1953 with the "C1" generation, until the most recent current "C8" generation. Every 5-10 years when a major drivetrain or body style change is made, the generation changes to the next "Cx" number. C1 through C7 generations all had front engine layouts, whereas the newest C8 generation has a mid engine layout. This simply refers to where the engine is positioned along the length of the vehicle, affecting the drivetrain layout and weight distribution.

Figure X: The 1997 C5 Corvette used for the project build

Our specific C5 generation Corvette came stock from the factory with a 5.7 liter displacement "LS1". "LS" refers to a widespread family of small block V8 engines produced by General Motors (GM) from 1997 to the present. Small block V8 simply means that they are a smaller displacement than the "big block" version, and V8 refers to eight total cylinders in a "V" formation of four cylinders per side.
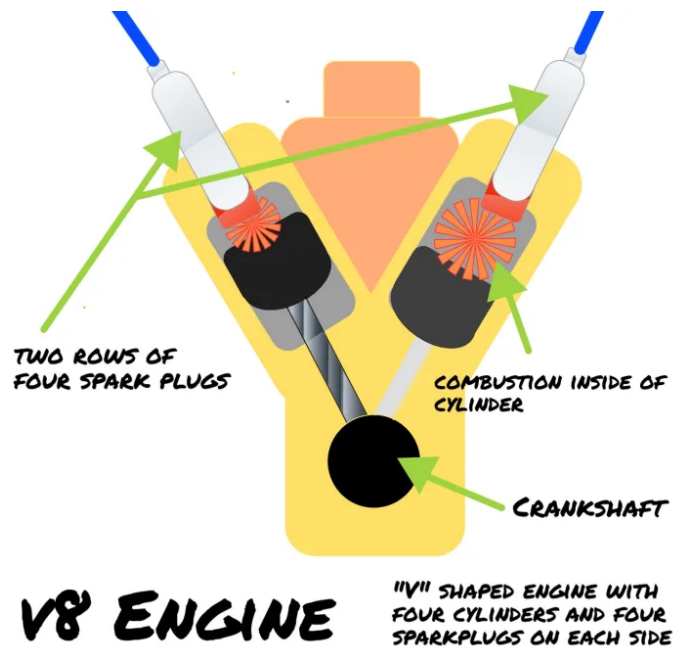
Figure X: V8 engine layout

Over the past 2 decades, various design changes and technological improvements have been made to increase power output, efficiency, and to be adapted to fit in various vehicle models. When major design changes have been made to the engine, the engine code changes to "LS2", "LS6","LSX" etc. The LS1 engine model comes from the 3rd generation Chevy small block. These came from the factory in GM vehicles such as 1997-2004 Corvettes, 1998-2002 Camaro, Firebird, Trans-Am, and various others. Additionally, in other vehicles, such as trucks and SUVs, engine blocks such as the LQ4/LQ9, LM4, and L33 were found. These blocks were identical to LS style blocks, some being aluminum and some being cast iron. As time progressed, the 4th generation blocks were introduced. These were slightly reworked blocks with more features. Similarly, identical blocks could be found in trucks and SUVs.

Basic Internal Combustion Engine Operation

The basic function of a four-stroke combustion engine involves 4 main stages. First, an intake-stroke, which occurs after the opening of the cylinder valves, drawing in a specific mixture of air-to-fuel into the engine cylinder as the piston moves down the bore. On the second-stroke, the piston reverses direction and begins compression. As the piston begins its journey back upwards, the valves are closed. During these first two strokes, the crankshaft makes one revolution. In the third stage, known as the "power-stroke", the air and fuel mixture ignites, causing a controlled explosion, forcing the piston to move down. Lastly, the piston moves in an upward direction as the exhaust valve opens, expelling the exhaust from the cylinder, thus completing two-full revolutions of the crankshaft.

Intake　　**Compression**　　**Power**　　**Exhaust**
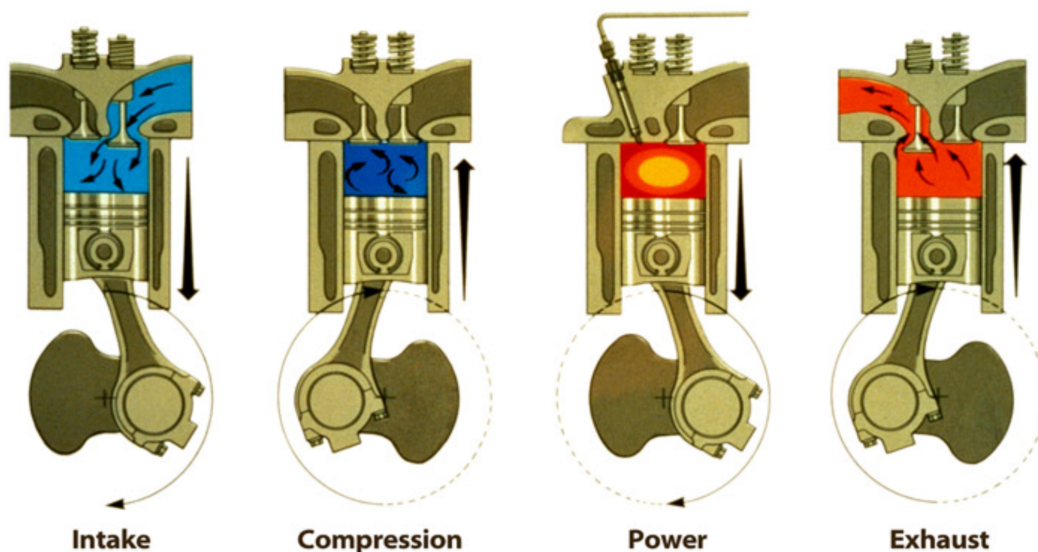
Figure X: Four cycles of an engine

The more air flowing into an engine, the more fuel that can be burned as a result. Airflow can be limited for a variety of reasons, including restrictions in both the intake and exhaust passages, as well as the closing and opening of valves to the cylinder. Air entering the engine enters at normal atmospheric pressure in a non-supercharged engine. The ratio of incoming air to fuel in most engines in pounds per square-inch is respectively 14.7 to one. This ratio can change during wide-open throttle where maximum power can be achieved, where the air pressure may slightly decrease.

The Air Intake System

While the majority of power gains in an engine occur from the components listed above, there are a multitude of ways to increase airflow to these components in both the engine internals and externals. In many cases this revolves around the inclusion of aftermarket parts that increase cross-sectional area of the many passages of fluids and reduce restrictions throughout the system as well as ways to manually increase flow. Technological advancements continue to find new and innovative ways to improve the process as well. When considering air intake, there are many ways to modify components before reaching the cylinders that can greatly increase flow in a responsible manner.

Air Intake Filter

The first functional component when considering the intake of air into an engine is the air intake filter itself. The main responsibility of this part is to filter out dirt and other foreign particles in the air or that may find their way under the hood of a vehicle and prevent them from entering inside the engine. There are two main-types of filters: an open pod or drop-in filter, where the open pod sacrifices lower filtration capabilities for better flow. Modifications may be necessary to intake passages to allow fitment of open pod intakes which makes the drop-in filter desirable for those looking for a simple replacement. The modifications in the passages may also allow for less bends in the piping which lower air pressure. Nevertheless, when considering ways to allow maximum airflow, the open-pod will always be desirable and still provide adequate filtration of debris. The diagram below elaborates on how the two types of intakes vary and will affect the fluid flow.
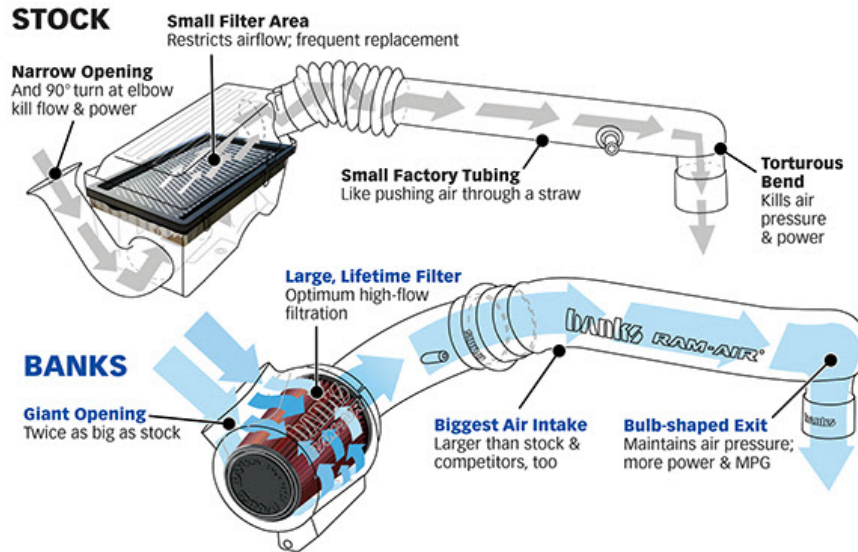
Figure X: Comparison of drop-in vs. open-pod air intake filters

Throttle Body

Following the entrance of air into the intake system, the volume of air then needs to be controlled. This occurs with the adjustment of the throttle. The throttle pedal, at the driver's right foot, is directly connected either via a physical cable, or a wire to the throttle body. The throttle body houses a plate that opens and closes as the throttle pedal is pressed down. The farther the pedal is pushed, the more the throttle plate is opened. At idle, the throttle plate is partially cracked open, allowing some air to flow and keep the engine running at low RPMs.

Figure X: Throttle Body with Throttle Plate

Intake Manifold

Next in the intake system is the intake manifold. The intake manifold's purpose is to evenly distribute air to each of the cylinders in the engine. The intake manifold houses individual runners, which feed each cylinder the same volume of air. When the engine is running, only one runner has air flowing through it during each stroke. This is due to air only entering into one cylinder at a time, as only one cylinder's intake valves are open. This causes vacuum in that runner, as the air is sucked into the cylinder.

Figure X: LS6 Intake Manifold

Forced Induction

In forced induction engines, a compressor is used to "force" air into the engine to increase power. A compressor driven by a belt or gear-drive is known as a supercharger whereas a turbine-driven compressor placed in the exhaust system is known as a turbocharger. Some losses will be generated to drive these compressors, however the overall power gains as a result of their integration are significant. A properly designed system will allow for higher boost pressures than exhaust, essentially forcing exhaust gasses out as well as cooling valves and completely filling the cylinder with air. Pressure relief mechanisms may be integrated into the system as well to prevent dangerous buildups of high-pressure air, helping avoid catastrophe within the engine.
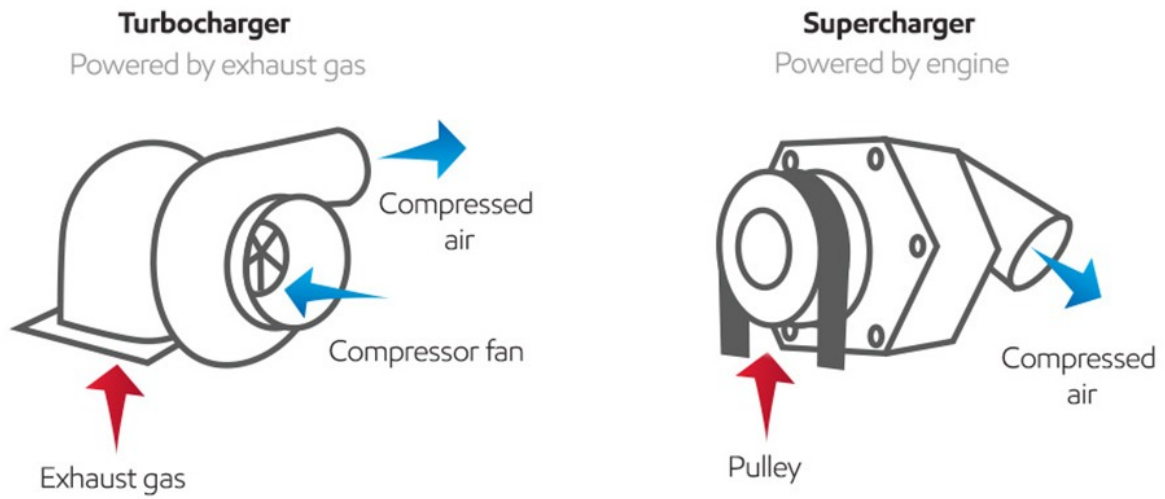
Figure X: Diagram differentiating turbocharger and supercharger function

Cylinder Heads

Camshaft

Camshafts are one of the most important parts of an internal combustion engine. They allow the valves to open and close. When valves open, gasses are able to enter and exit the combustion chamber. Each cam lobe controls one individual valve. If an engine has 16 valves, there must be 16 cam lobes. At the cam lobe peak, the valve is completely open, and at the opposite end of the cam lobe, the base circle, the valve is completely sealed shut. Camshafts are typically made from either cast iron or billet steel. They are usually driven by a belt or chain, although some applications use gear driven camshafts as well. Whichever method is used to spin the camshafts, it is imperative that any camshaft found within a motor spins at the exact speed of the crankshaft. This accounts for engine timing, as the valve must open and close at the correct moment to allow for optimal combustion at the stoichiometric ratio of air to fuel.

Figure X: V8 Camshaft

Pushrod Style Engine

Pushrod style engines have their camshaft located within the engine block, right above the crankshaft. It utilizes pushrods which push on rocker arms to open and close valves. These engines, in V formation, are typically less wide, meaning they can fit in engine bays easier, with more room along the sides. Additionally, they are more simple, and the designs have been around for centuries. GM's LS series engine, a pushrod style engine, is used in almost all larger GM vehicles, meaning it is easily accessible.
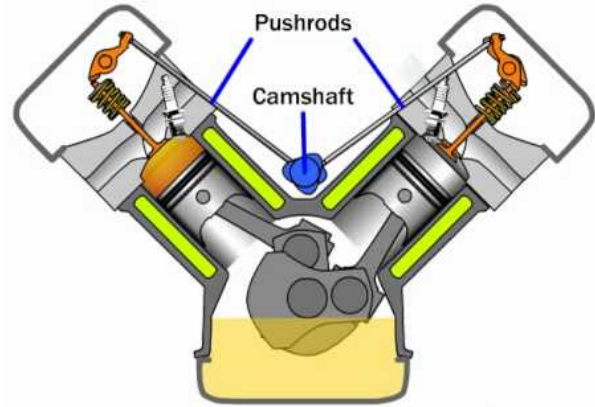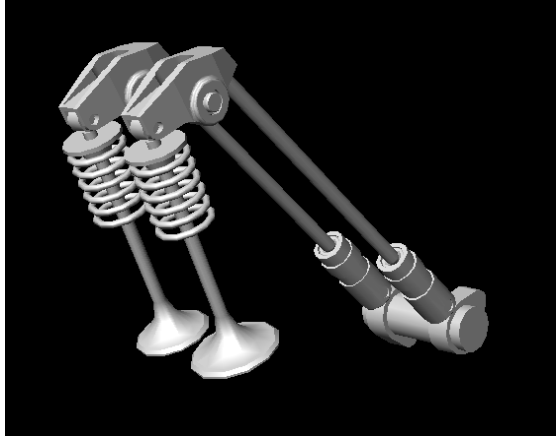
Figure X: Diagram depicting pushrod style orientation

Overhead Camshaft Style Engine

Overhead camshaft style engines have their camshaft(s) located in the cylinder head as opposed to inside the engine block. The camshaft pushes directly on the valve without the need for pushrods. There are both single overhead camshafts and dual overhead camshafts. Single overhead camshaft engines, similar to pushrod engines, use one camshaft to operate both intake and exhaust valves. Dual overhead camshaft engines utilize an intake camshaft and exhaust camshaft, which operate their own respective valves.

Figure X: Diagram and image depicting overhead style orientation

Exhaust System

After the combustion occurs within the cylinders, the waste gasses must evacuate the engine. The purpose of the exhaust system is to evacuate these exhaust gasses efficiently by routing them underneath the vehicle (typically to the rear) through hollow metal piping. The exhaust system is also an important aspect of optimizing air flow, because the air cannot be taken into the engine until the combustion gasses have left the engine. Other purposes of the exhaust system include housing oxygen sensors, converting some of the toxic pollutants into less harmful gasses, and reducing volume output.

Exhaust Manifolds

In a similar fashion to the intake manifold where air is evenly distributed to each of the cylinders, exhaust gasses are collected from the cylinders and funneled out through a single opening in what is called the exhaust manifold. With that, increasing the size of the passages in the exhaust manifold will allow for increased fluid flow, similar to the intake system in that there are less restrictions to the flow. These manifolds are generally cast-iron or stainless steel units as they must be able to handle the high heat of the exhaust gases as they exit the engine, whereas intake manifolds house much colder air and can be composed of plastics.

Catalytic Converters

After air flows through the exhaust manifold the second element of the exhaust system is the catalytic converter. This component is responsible for making toxic pollutants less toxic in nature through catalyzing a redox reaction and converting them to less harmful pollutants such as carbon dioxide or water vapor. These parts can be very valuable as oftentimes precious metals are used as the catalyst and coats the inner-honeycomb structure of the converter. Airflow can be optimized through this part by simply integrating a high-flow performance catalytic converter into the exhaust system, which would possess a looser honeycomb structure allowing for less restricted flow.

Rear Piping

The final components of the exhaust include piping that runs from the catalytic converter to the rear end of the vehicle where the exhaust gases fully exit the system. Throughout this piping there may be numerous silencing pieces known as mufflers and resonators to help control the noise output coming from inside the engine. These silencers are finely tuned to reflect sound waves produced from within the engine to cancel out the sound. The issue that may arise with these components when considering air flow is they may pose some restrictions to this flow. Once again, integrating high-flow components can help to reduce this issue or eliminate them all together, however in many states that option will not comply with emissions rules and regulations. However, the best flow will be achieved with solely exhaust piping from the catalytic converter all the way back to the exit of the exhaust gases. A diagram of a typical exhaust system with many of the components mentioned in this section compared to a racing-style system where airflow is optimized can be found below.

FACTORY EXHAUST SYSTEM
Most factory exhaust systems include cast exhaust manifolds, one or two catalytic converters, a resonator and at least one muffler.

MUFFLER   BACK PIPE   CATALYTIC CONVERTER   EXHAUST MANIFOLD

CATTED PERFORMANCE EXHAUST
Some aftermarket exhaust systems replace the factory catalytic converters and resonators with high-flow versions to maintain the vehicle's street legality.

MUFFLER   BACK PIPE   CATALYTIC CONVERTER   EXHAUST MANIFOLD

RACING EXHAUST SYSTEM
Full racing exhaust systems completely eliminate catalytic converters and resonators with straight-through piping for maximum unrestricted performance.

MUFFLER   BACK PIPE   STRAIGHT PIPE   EXHAUST MANIFOLD

DSPORT
PERFORMANCE + TECH MAGAZINE

Figure X: Comparison of factory vs. performance and racing-style exhaust systems

Vehicle Drivetrain

Clutch

Torque Tube

Dynamometers

A dynamometer, or dyno, is a measurement device used for calculating moment of force; or torque, as well as power outputs. There are numerous applications for dynamometers, however when being used in an automotive application, the power generated by an engine can be calculated using the torque and rotational speed of the engine. To derive the power from the measured torque, the rotational speed in rpm of the engine is multiplied by the torque output and the product is divided by 5,252. Dynamometers can be used to get power measurements and sensor readings from the car, but it is more commonly used to tune engines for peak performance, economy, or driveability.

The key feature of a dyno is that it is able to simulate driving as if you were driving normally on the street. Without this load provided by the dyno, the engine and drivetrain would not have any resistance while accelerating. The load is needed to simulate the forces an engine has to overcome while driving on the street: the force needed to propel a several thousand pound object, the force of friction within the engine, drivetrain, and the tires in contact with the road, as well as the air resistance that increases with speed. A dynamometer can actually simulate more load on an engine than it would typically endure on the street. The load decreases as the speed increases due to inertia typically, but this is not the case on a dyno. A dyno can load an engine more at a far lower rpm, as the acceleration is not limited by spinning the tires or stalling a torque converter, as it might while driving on the street. Much of our data will be collected with a dynamometer; torque and horsepower output will be the most important unit of measurement we will gather from the dyno, however all engine parameters will be measured as well.

The data is calculated by the dyno through a data acquisition system consisting of both a commander and workstation component. The commander is often simply a computer that will send commands to the workstation, a software that can then operate the load and throttle control systems. The data is then collected and sent back to the commander where it can be processed, analyzed in the form of graphs or charts, and stored for future use. By providing the user with a graph of horsepower and torque output in addition to air/fuel ratio parameters, intake air temperatures, and many other sensor readings, the user can adjust some of these aspects in the ecu to achieve the desired goal. A dyno allows the user to see the parameters and outputs as well as test the car through the engine's rpm range with a load on it, to simulate driving on the street.

Types of Dynamometers

There are four types of dynos that are typically used in industry. The most common type of dyno is the inertia dyno. Following is the water-brake dyno which is the next most common dyno used. The next most common is the eddy brake dyno, which is more expensive but does have some advantages over the water-brake. Finally, the least common type is an alternating current (AC) dyno. AC dynos are more expensive than the other types so they are reserved more for high end programs such as F1.

Inertia Dynamometer

Inertia dynamometers are the most common type of dyno that is used, especially in an aftermarket setting. These dynamometers work by driving the vehicle's driven wheels onto large, heavy rollers and accelerating at wide-open throttle. The dyno only reads information taken by the rate of change of acceleration, hence the name "inertia" dyno. The dyno software calculates the power based on the roller velocity and the time needed to achieve a certain rate of acceleration. These values are found using sophisticated accelerometers and computer software. Inertia dynos operate based on Newton's second law of inertia, where the rate of acceleration is directly proportional to the power placed on the heavy rollers by the tires. Dynojet is a popular brand of dynamometers and is the most common pure inertia dyno used in the automotive industry. Inertia dynos are objectively more simple than other types of dynos, however there are some disadvantages to this design. Firstly, these dynos cannot adjust the resistance of the rollers to accurately reflect the weight of the specific car on the rollers. Also, inertia dynos may not allow turbocharged engines to build boost as it would driving on the street, which is a big disadvantage when tuning turbocharged engines that require utmost precision with regards to fuel and timing in order to prevent the engine from failure. Finally, one of the most notable drawbacks with an inertia style dyno is the limitations of tuning. Inertia dynos are used for wide open throttle acceleration and cannot do load or step tests. With this limitation, it is harder to tune the engine under different loading conditions, such as street driving or holding a constant speed on the highway. Only being able to get results under wide open throttle applications makes it difficult to optimize the timing and fuel curves for the engine for efficiency, power, and driveability.

Water-brake dynos, or hydraulic dynos, differ from inertia dynos in that they use fluid, hydraulic fluid or water, to provide braking force on the dyno to more accurately load the engine in various scenarios. These dynos utilize a constant speed brake as well as a rotor with a stationary and rotating component. The rotating mass component of the rotor (the rollers that are being spun by the wheels) stores energy and provides an initial inertial mass that must be overcome. In addition to the initial force needed to overcome the roller inertia, the dyno software calculates the additional load needed at any point in time. The rotor elements generate the braking force needed to load the engine with hydraulic fluid or water. The braking force generated by the rotor aims to match the output of the powertrain on the dyno. To measure the torque, the dynamometer utilizes a strain gauge to determine the torque reaction between the rotor's stationary and rotating elements. From this reading, an engine's horsepower can be calculated by the dyno. Although hydraulic dynos are capable of simulating various driving/racing conditions unlike an inertia dyno, there are still limitations to the machine. The most notable drawback with a water-brake dyno is the delay between stepping on the throttle and

Mention Dynapack

Eddy Current Dynamometer

An Eddy Current is an electromechanical energy conversion device that fundamentally uses Faraday's law of electromagnetic induction to function. An Eddy Current dyno (sometimes referred to as an Eddy Brake dyno) uses the Eddy Current to measure dyno readings and provide the loading necessary for the dyno. These types of dynos have fewer energy losses, higher efficiency, and are more versatile than traditional mechanical dynamometers. The fewer losses are due to the absence of any physical contact between windings and excitations inside the eddy brake. The friction in these dynos is almost negligible compared to traditional dynos.

The vehicle is put on the dyno by being strapped down to planted elements of the device and placing the wheels of the vehicle on rollers in which the car can accelerate, yet remain stationary on the device. The car is then accelerated up to a certain number of engine revolutions per minute (RPM), which varies depending on the vehicle and dyno purposes. Following the run, the data acquired from the dynamometer can be processed and analyzed on the commander.

Simulation Software

Since our primary goal is to find which upgrade has the greatest effect on power development, we thought that it might be interesting to try to predict where the gains come from. Doing so is no easy task. Even with some approximations, the thermodynamic conditions surrounding an engine are complicated. The environment of the engine and the load it experiences are the two top-level variables that need to be simulated. Then there are material properties, component geometries, and turbulence characteristics that need to be determined. The complicated thermodynamic situation surrounding the engine and which upgrades will impact performance cannot be easily resolved by-hand.

Currently, the best way to model fluid flow is with computational fluid dynamics (CFD) software. CFD software models the complex thermofluid situation inside or around a particular geometry. All CFD software packages try to solve the partial differential equations known as the Navier-Stokes equations. These equations model the conservation of mass, momentum, and energy of a control volume. A control volume is an infinitesimal volume that compliments the partial differential equations. The total volume of fluid being analyzed using the Navier-Stokes equations has an infinite number of control volumes, thus making the domain of the analysis continuous.

In theory, this is an elegant way of conceptualizing the situation, but CFD software cannot analyze an infinite number of control volumes. So, a researcher applies a mesh to the geometry to discretize the domain. The mesh creates control volumes that the solver uses to balance the Navier-Stokes equations. The solver solves them based on boundary and initial conditions for the fluid volume as well as numerous other characteristics. The accuracy of the solution is highly dependent on the quality of the mesh. A larger number of cells (analogous to

control volumes) will yield more accurate results but increase the time it takes for the solver to converge to a solution. But, the shapes of the cells also impact the accuracy of the solution. A good cell is regular in size and shape, and is not stretched or thin. Complex fluid volume geometries can cause cells to become irregular. CFD software usually includes a meshing tool to create a mesh with many parameters that can be tweaked to improve the mesh geometry.

Many theories have been developed to model fluid flow in all types of temperature, pressure, and velocity regimes. CFD software packages include ways to change the model type to fit the regime that is being tested. For this project, we are primarily interested in the fluid flow interaction inside of a part. There is only one phase and one type of fluid, the flow is turbulent, and the material properties of the fluid are not constant. These are all parameters that CFD software packages have control over. For this model, the most interesting of the parameters is the viscous model type. The viscous model of the fluid determines how the solver handles turbulence. Turbulence is the small scale change of the velocity of a fluid. Whether a fluid is turbulent or laminar is related to the Reynolds number of a fluid. The Reynolds number, a dimensionless quantity, is dependent on material properties (themselves a function of temperature and pressure), flow velocity, and geometry. Researchers have developed numerous turbulence models to fit a variety of operating and mesh conditions. Thus, the solver can model the flow conditions inside our parts tailored to our operating environment.

CFD modeling is an important way to conduct tests on parts in research or industry. Having a way to accurately model fluid flow in or over a part means that researchers or engineers do not have to create prototypes and expensive testing apparati. Prototypes and test setups are expensive to create and are rigid in their purpose. If the prototype were made incorrectly or needed to be changed, then a new prototype would need to be made. Testing apparati may also need to be changed if a new prototype were developed. These processes take time, and depending on the application this could be weeks or months of waiting. CFD has the distinct advantage of being quickly adaptable to new situations and parameters. The researcher or engineer only has to rerun the CFD model with the new conditions to produce a new test result.

Modeling this way implies, though, that the underlying relationships accurately portray the world in simulation. This assumption is not valid. Much of what scientists and engineers know about thermodynamics and fluid flow is based on ideal theories and empirical relationships. These are usually bound within some range of temperature, flow type, flow material, pressure, etc. Nature ignores these boundaries and can transition a fluid between different models depending on the conditions. However, this flaw in CFD modeling should not detract from its value. CFD is useful for quick and varied models especially in the initial stages of testing. CFD can be used to show scientists and engineers where to focus their efforts and to eliminate poor designs without having to manufacture the prototypes and create the testing apparati.

Objectives

Methodology

Engine and Internal Components

The group spent extensive time discussing our project goals and what modifications were necessary to get there. Aside from simply increasing airflow to increase the power output, many other modifications were necessary in order to ensure the engine was able to withstand the increased forces by the increased power. These are commonly known in the automotive world as "supporting modifications", and allow the engine to not only make a higher power, but to make that higher power reliably without failure. As with everything, higher performance parts are more expensive due to various material, processing, and engineering improvements as will be discussed in detail for each component. As the group was working on a budget and spending a considerable amount of money out of our own pocket, the build components had to be selected carefully and strategically. Our group had to analyze each component to balance where it was possible to save money, with where it was crucial to spend the extra money. If they were to fail, the majority of these components would cause "catastrophic failure" to the engine. This means the engine would be unable to operate and further irreversible damage to many of the other components would result-sending thousands of dollars down the drain.

After extensive planning and parts purchasing, and performing initial testing on the stock engine to establish baseline power numbers, work began on the new engine build. In addition to assembling the components throughout the engine overhaul, machine work and balancing was necessary and was all performed by ABT Machine Company in Holliston, MA.

Engine Block

The LS1 engine block is made from cast 319-T5 aluminum, has eight cylinders at a 90° cylinder angle, and 5.7L of displacement with a compression ratio of 10.2:1. The 3.90" diameter bores are spaced 4.400" on center with a stroke of 3.62".

The engine block that is being used for our project build is called an LQ4, sometimes also referred to as a Vortec 6000. LQ engines are also small block V8's produced by GM, however these were used in GM trucks from 1999 to 2007 such as the Silverado, Suburban, Yukon, Sierra, and various others.

The LQ4 engine block is made from cast iron, which is more dense, stronger, and can handle higher temperatures than the stock LS1 cast aluminum block. Although the density of iron does mean this block is about 75-100 lbs heavier than the original block, its increased strength is necessary to reliably withstand the elevated forces and stress due to the increase of horsepower without risk of catastrophic damage. Since the LQ4 engine also has eight cylinders at a 90° angle and are spaced 4.400" on center, it is compatible with many factory LS engine components and is a good candidate for our build. The LQ4 engine has the same stroke length at 3.622", but has larger pistons at 4.000" in diameter for a total displacement of 6.0L. This 0.3L increase in displacement allows for more fuel to be drawn into the combustion chamber, leading to an increase in power output by the engine.

Summary of Engine Block Differences		
Property	LS1 (original)	LQ4 (our build)
Material composition	Cast 319-T5 aluminum	Cast Iron
Cylinders/layout	V8	V8
Cylinder orientation	90° angle, 4.400" on center	90° angle, 4.400" on center
Bore diameter (stock)	3.900"	4.000"
Bore stroke (stock)	3.622"	3.622"
Displacement (stock)	5.7L	6.0L
Compression ratio	10.2:1	9.4:1

Table X: Engine Block Comparisons

After sourcing our LQ4 engine block, it was sent to ABT Machine Company to be prepared for use in our build. This included thermal cleaning, magnafluxing, honing the cylinder bores to 4.0055" diameter, decking the cylinder head mating surfaces to 9.225". This work essentially takes a 20 year old used engine and prepares all the engine surfaces and features to proper finish and size tolerances to be used in operation for our build goals.

Figure X: Machined LQ4 Engine Block

Crankshaft

The stock crankshaft in both the LS1 and the LQ4 engines are both cast iron and capable of withstanding the forces of 1,000 whp. Aftermarket options such as forged 4340 steel crankshafts do exist to withstand even higher power, but are unnecessary and not cost effective for the goals of our build. Therefore, the stock LQ4 crankshaft was reused after being cleaned and magnafluxed by ABT.
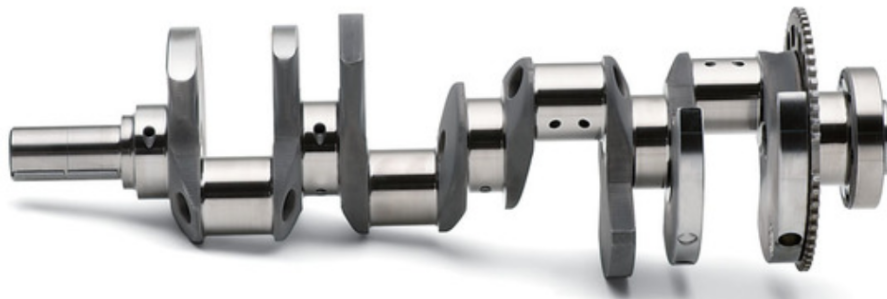
Figure X: Stock LS1 Crankshaft

Main Caps and Bearings

The crankshaft is secured into place in the block by the main caps, or "mains" as they are commonly referred to. Main bearings are inserted into the block and the main caps, which clamp around the main journals of the crankshaft to secure it when the mains are tightened down. The stock LQ4 mains are made of ductile steel and capable of 1,000 hp, so upgrading to billet steel mains is unnecessary for our build goals. The LQ4 engine has five "6 bolt mains". This means there are five total main caps, one on each end of the block and then one between every pair of cylinders, and each main is secured by six bolts.
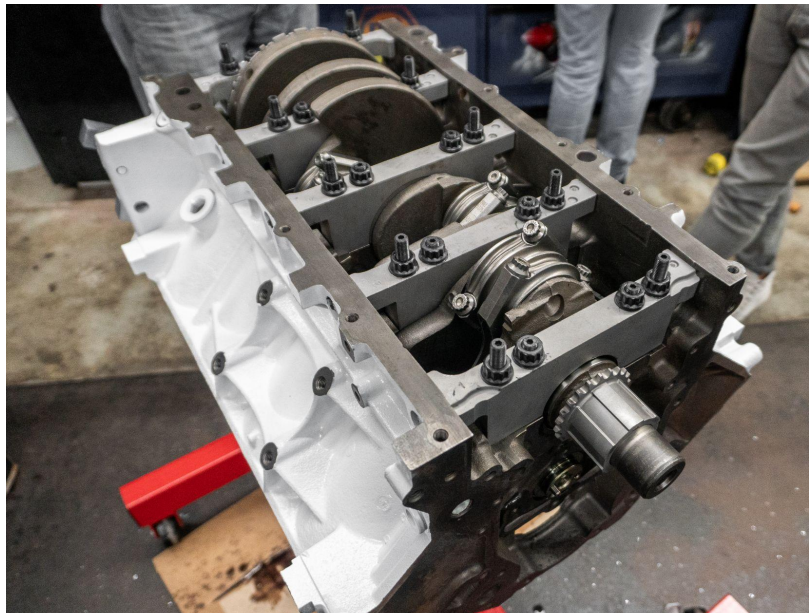

Figure X: Main caps assembled to secure crankshaft

Each main has four traditional bolts securing it from the top down, and then two additional bolts, one from each side.These main bolts were upgraded to ARP M10 main studs in order to better secure the main caps and in result prevent any unwanted movement from the crank under high power/RPM. Studs work in the same way as bolts, however instead of having a head that is turned by force to rotate the entire bolt into the threaded hole, they are threaded in freely and then a nut is threaded on and tightened. Since the studs do not turn during the tightening, (only the nut is turning onto the stud) the stud is being torqued from a relaxed state. This means that the stud is only experiencing tensile stress and stretching in its longitudinal axis, rather than a bolt which is also subject to torsional stresses and under the twisting load. The result is a more reliable and consistent securing force due to a more equally distributed load and a more accurate torque value. Additionally, ARP stands for "Automotive Racing Products" and is a company who specializes only in fastening hardware for automotive use. ARP uses their specially developed and patented 8740 chromoly steel alloy for these studs which has superior mechanical properties compared to the stock grade 8 bolts. The main bearings allow the necessary free rotation of the crankshaft while still providing the adequate support to keep the crankshaft in position. The stock main bearings are more than sufficient for the goals of our build.

Figure X: ARP Main Stud, Nut, and Bolt

Connecting Rod Assembly

The connecting rods, or "rods" are clamped around the crankpin journals on the crankshaft at the "big end" by two rod bolts, and attached to the pistons at the "small end" via the wrist pin. As discussed earlier, each combustion within a cylinder chamber is an explosion which forces the piston towards the center of the engine during the "power stroke". The rods are responsible for connecting the piston to the crankshaft to transfer that linear motion in the cylinder to rotate the crankshaft. This means that as the power of the engine is increased, they must withstand higher and higher forces at elevated temperatures without deformation.
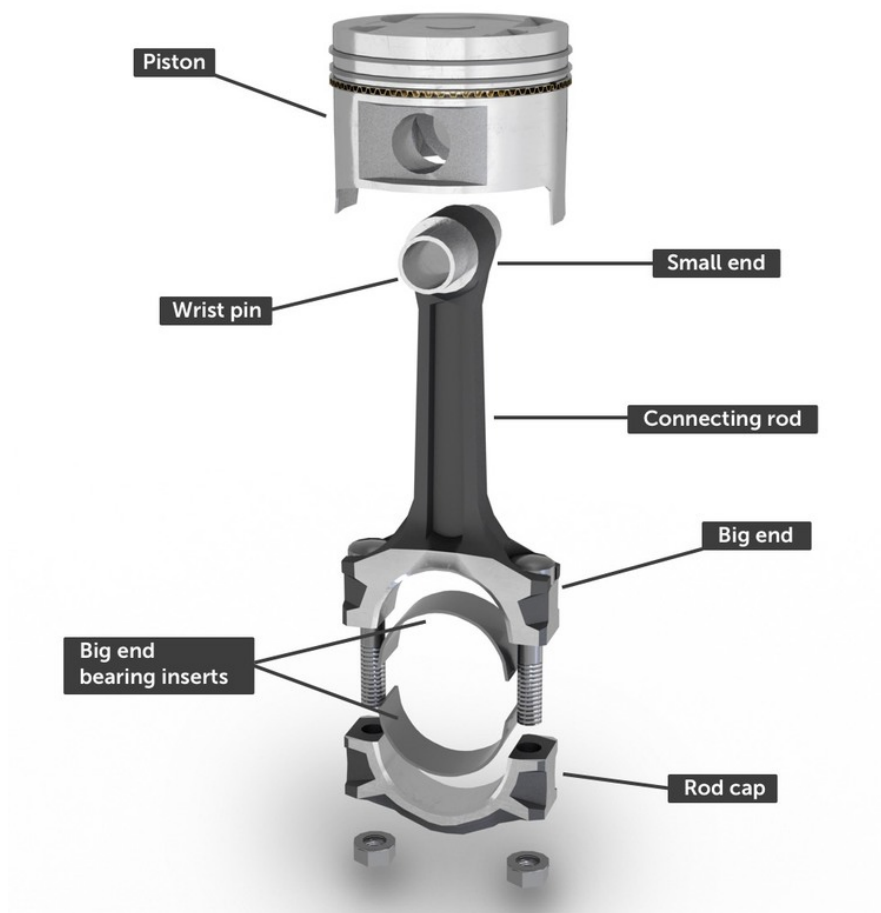

Figure X: Labeled Diagram of Connecting Rod Assembly
(piston shown for reference)

Both the LS1 and LQ4 engines use the same powdered metallurgy "I-beam" design connecting rods. Powder metallurgy is the process used to manufacture the shape, dimensions, etc. of the rods from their raw material. Specifically this includes taking the powdered metal particles and any additives, compacting it to the desired shape, and applying heat or pressure (sintering) to create a solid part without heating it above the melting point. Secondary machining and finishing processes are often done for critical features that interface with other parts. The "I-beam" design refers to the linear cross sectional shape of the connecting rod, similar to a steel "I-beam" used in building construction.
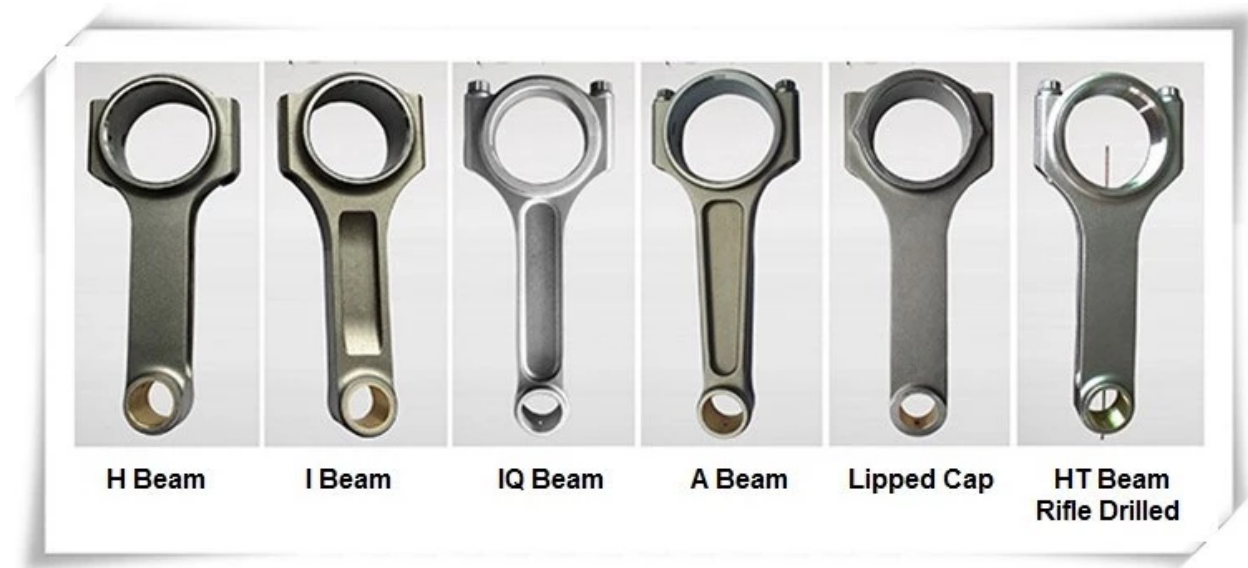
Figure X: Diagram of different rod designs

Due to our power output goals when optimizing the airflow, it was necessary to upgrade the stock connecting rods to aftermarket ones to withstand the much higher force and stresses. There are extensive aftermarket options for rods, and after research for an adequate balance between price and performance, our team decided to use Eagle Specialty Products H-Beam Connecting Rods. These are an H-beam design of forged 4340 steel with an advertised rating of up to 1,300 hp and 7,500 RPM, compared to the stock rods and bolts of about 500 hp and 6,500 RPM. This substantial increase in capacity is due to the improvements in connecting rod material, design geometry, and rod bolt material.

Figure X: Eagle Specialty Products H-Beam Connecting Rods

In addition to using a specialty high carbon steel with superior material properties, with the forging manufacturing process the grain flow of the material is able to be controlled in order to flow with the part shape, in this case the connecting rod. This results in a more uniform and predictable grain structure to increase the directional strength, as well as reducing internal voids and offering better response to heat treatment. After forging, the Eagle H Beams are multi stage heat treated, X-rayed, sonic-tested, magnafluxed, 100% machined, and shot peened to stress-relieve the material (quote from Summit Racing). Through the forging, secondary processes, and elevated quality control by Eagle these rods gain substantial mechanical properties for their application in an engine under higher horsepower.

The Eagle H-beams have an H-beam design rather than the stock I-beam design from GM. I-beam design connecting rods can be better under compression forces, so they are a good choice when running very high amounts of boost which greatly increases compression forces. However, our engine build will not be subject to very high amounts of boost (only 12-15 psi), and the H-beam design is able to save weight compared to the stock rods while still handling the power. Each of these Eagle H-beams are 620 grams compared to the stock rods at 650 grams, saving 30 grams per rod for a total of 240 grams. Since these rods are part of a rotating mass, weight savings become very significant to reduce the force needed to rotate the crank and

produce power. Additionally, reducing weight in the rod and piston reduces the tensile forces the rod is subjected to and they are not tapered, which improves support at the wrist pin end.

Rod Bolts

These Eagle H-Beams also come standard with ARP 2000 rod bolts, used where each rod is clamped around the crank pin journal by the two rod bolts. These rod bolts are made from their specialty ARP 2000 alloy, which as discussed previously is far superior to the stock rod bolts and is rated to 230,000 psi and helps withstand higher RPM.

Figure X: ARP 2000 Rod Bolts

(mock installation without crankshaft for reference)

Pistons

Pistons are especially crucial to an internal combustion engine build because they are the closest component withstanding the elevated temperatures and forces due to the combustion of fuel in the cylinder chamber and the pressure from combustion gasses. As previously discussed, while increasing fuel and air flow comes with increasing combustion forces, the pistons in our build must be able to withstand this. The stock LQ4 engine comes with "dished" pistons made from M124 hypereutectic cast aluminum alloy. Dished (as opposed to flat top) refers to a style of

pistons where there is a "dished" indentation in the top face (combustion side) of the piston that allows for valve clearance and reduces the compression ratio since it adds volume to the compression chamber compared to a flat top. These pistons would not reliably withstand the forces of our boosted application, so they were chosen to be upgraded to Summit Racing Pro LS Forged Pistons.

Figure X: Summit Racing Pro LS Forged Pistons

These upgraded pistons are forged from premium 2618 aluminum alloy. The M124 alloy used in the stock pistons is a proprietary metal made by Mahle and composition/specifications are not available to the public, however 4032 is the other widely used alloy for forged piston applications. The 2618 alloy used in the forged pistons we selected is a superior alloy mainly due to having a much lower (~12%) composition of silicon, which is replaced with a higher composition of aluminum, copper, magnesium, and a small amount of titanium. This results in an increase in mechanical properties that can be seen in the table below.

Piston Alloy Characteristics

Material Characteristics	4032	2618
Tensile Strength	55,000 psi	64,000 psi
Yield Strength	46,000 psi	54,000 psi
Fatigue Endurance	16,000 psi	18,000 psi
Modulus of Elasticity	11,400 psi	10,400 psi
Melting Point	990 - 1,060 F	1,020 – 1,180 F

Table X: Forged Piston Alloy Characteristics

Additionally, as previously discussed the forging manufacturing process produces much better mechanical properties as compared to a casting manufacturing process since forging allows for better control over grain orientation.

Piston Rings

Pistons have metal rings around their outer diameter that contact the cylinder wall, rather than the piston itself. Most four stroke engines use three rings, with the "top" (closest to top face of piston) two rings being responsible for forming the seal between the cylinder wall and the piston to maintain the pressure in the combustion chamber. The "bottom" ring (closest to the crankcase) is responsible for maintaining the adequate thin film of oil on the cylinder walls, which is necessary for proper lubrication to reduce the friction that could otherwise damage the engine by wearing out the piston rings or scoring the cylinder walls. The stock piston rings are plasma moly top rings and ductile iron 2nd rings. We used Summit Pro LS rings that are made in conjunction with the Pro LS pistons. These rings are also plasma moly and ductile iron, respectively, but are thicker than factory rings with the ringlands of the pistons enlarged for their

accommodation. The first piston rings are gapped to .024 inches and the second to .022 inches.

Figure X: Piston Rings Installed on Forged Pistons

Figure X: Engine block after installation of crankshaft, camshaft, piston and rod assemblies

Cylinder Heads

Figure X: Fel-Pro Cylinder Head Bolts

Engine Build Summary

The engine build consisted of factory components from various GM LS/LQ engines and aftermarket components purchased from automotive performance companies. Each component was selected specifically to satisfy the project goals and assemble a powerful yet reliable engine, and for clarity a summary can be seen in the table below.

Table X: Engine Build Summary

Supporting Drivetrain Modifications

Intake Manifold Flow Simulations

The original desire of the team was to simulate air flow through the entire intake system of the car. Quickly, we realized that this was a task too complicated for us to simulate with any accuracy. The intake air box, supercharger, intercooler, intake manifold, and cylinder heads together make a system which is incredibly dynamic and complicated. While it would be incredibly interesting to model this system, the project team would have to create each part and then test them together. So instead, we chose to focus our efforts on the simplest of the components: the intake manifolds. We decided to model the flow of air through each manifold for two revolutions of the engine. Since two revolutions correspond to four strokes, the simulation would model how air flow changes inside the manifold as different cylinders accept air.

Simulation cannot occur within a vacuum. Therefore, before any work could be done on the simulation model, the software platform through which flow was simulated had to be chosen. A number of CFD software packages exist that would work for this project. Software packages include ANSYS Fluent, Solidworks Flow Simulation, Autodesk CFD, OpenFOAM, and SimScale. All of these are developed CFD programs that solve the Navier-Stokes equations for imported geometry using a mesh, material properties, and operating and initial conditions. We chose to use ANSYS Fluent for this simulation for a few different reasons. First, ANSYS Fluent is specialized CFD software. It was built solely for CFD analysis unlike Solidworks or Autodesk which originally were solid modeling software. Second, WPI already has a license for ANSYS and its related products and it will run on their computers uninterrupted and protected unlike SimScale which is cloud-based software. Third, it is developed by experts who can maintain a steady level of support unlike the open-source OpenFOAM. And, like all of these software packages, solid modeling and meshing tools are included in the ANSYS suite of tools.

Every CFD simulation can be broken down into five top-level steps before results can be visualized. Geometry must be defined and imported, a mesh must be applied to the geometry taking into account the boundary layer regions, material properties must be defined, operating and initial conditions must be defined, and solver models and parameters must be chosen. We made many choices here to try to simulate real-life inside the software.

As was previously explained, we chose to use an LS6 intake manifold and a Trailblazer SS intake manifold with our engine. These manifolds have the same port size and fit onto the cylinder heads the same way. The geometry of the runners and plenum, though, are nowhere near similar. Initially, we looked for existing solid models of the intake manifolds. These parts were manufactured using a molding technique which did not imply that a solid model of the manifolds existed. We asked aftermarket manifold manufacturers if they had existing models of either of our manifolds. We believed at the time that the aftermarket manufacturers based their manifolds at least in part off of the OEM manifolds. However, our response from them was all the same: they had no models that they were willing to share if they had any at all. So, the next step was to ask GM ourselves. Unfortunately, after reaching out to their customer service department we learned that the models were not available from them either. So, to get our simulation data, we would have to make the solid models ourselves.

For our simulations, we needed to model the interior volume of our manifolds. We developed two potential strategies to be able to recreate them. Our first idea was to use a 3D scanner to model either the manifold itself or the fluid volume inside. This would have created a dimensionally accurate model of the manifold as long as the tool to create the scan could see inside the manifold. However, we were unsuccessful trying to find a scanner that we could use at WPI or at nearby universities. So, our second strategy was to make the solid models ourselves. This has the benefit of requiring no specialized equipment, but would require the team to dimension both manifolds very carefully and then translate those drawings into a solid model. Without any other options, this is the method that the team was forced to use in order to generate solid models of our manifolds.

For the initial simulations, we utilized a simplified model of an intake manifold for this engine. The model included eight runners that wrapped over top of the plenum and had outlets at an angle. Figure X shows the simple geometry manifold that was used initially. This simplified model did well to test different parameters within ANSYS since simulations converged quickly. This way, the parameters of the solver could be tweaked while the development of the solid models occurred in parallel.
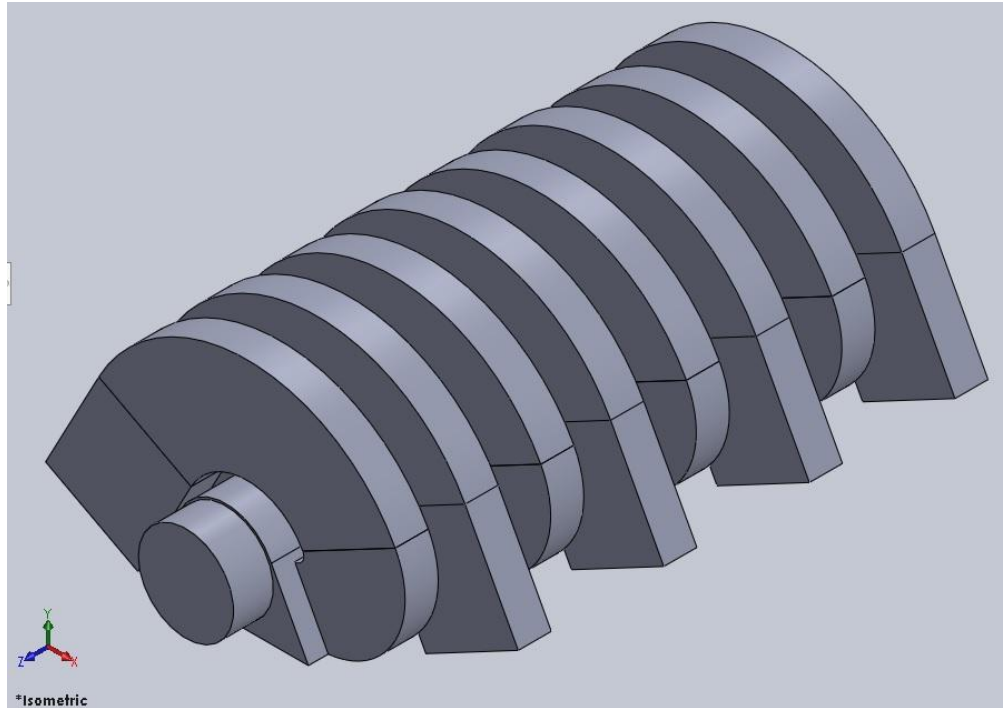
Figure X: Rapid Testing Manifold Geometry

The team meticulously dimensioned each manifold so that they could be recreated within Solidworks. Certain features were ignored and smoothed to simplify the measurements and the solid model geometry. Since CFD modeling is not perfect, simplifying the geometry is an acceptable tradeoff and improves the convergence speed of the solver. The team created three versions of the LS6 manifold and two versions of the Trailblazer SS manifold before we deemed them accurate for our simulations. Figures X and X show the final version of the manifolds that were used. Appendix A contains the figures showing all versions of each manifold variation.
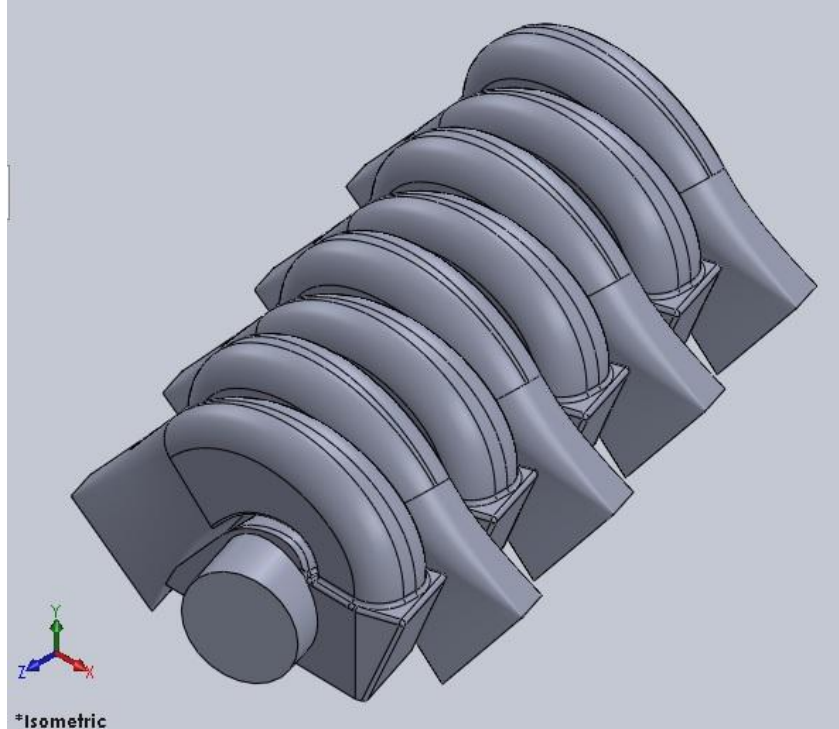
**Figure X**: LS6 Intake Manifold Interior Volume Solid Model
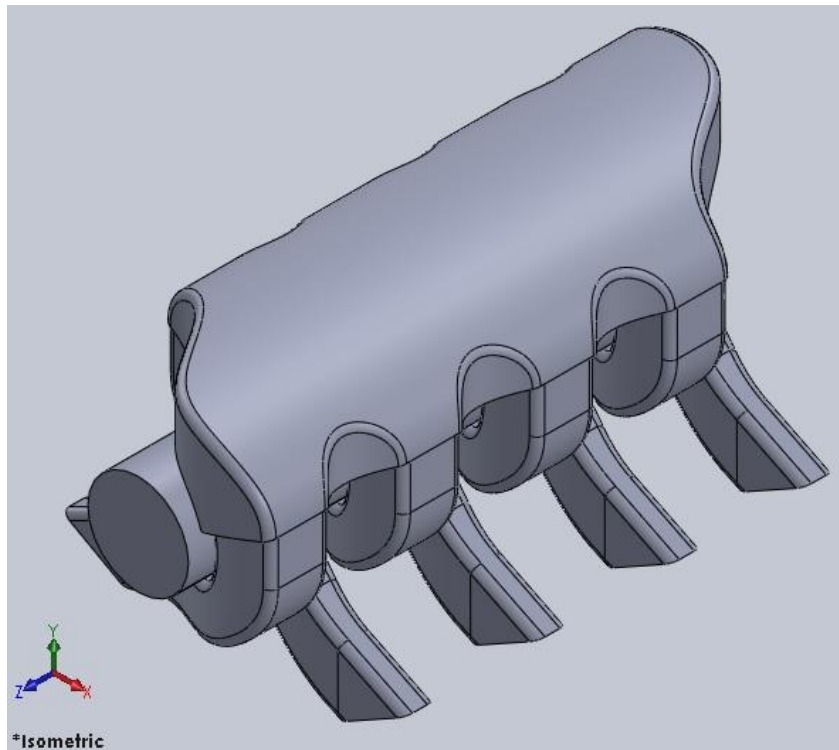
Figure X: Trailblazer SS Intake Manifold Interior Volume Solid Model

Figure X shows the main interface of ANSYS with Fluent ready to be used by the user. Different modules within ANSYS perform different functions. The only one that we used directly was ANSYS Fluent. ANSYS provides a few different versions of CFD software. We chose Fluent specifically within ANSYS because Fluent works well with pipe flow. Fluent contains five cells that contain information about the geometry, mesh, setup, solution, and results of the CFD model. The geometry, mesh, and results cells open other tools within ANSYS, but the remaining cells use Fluent directly. The cells interface with each other, and any updates to a cell higher on the list is captured and requires the user to rerun the subsequent steps.
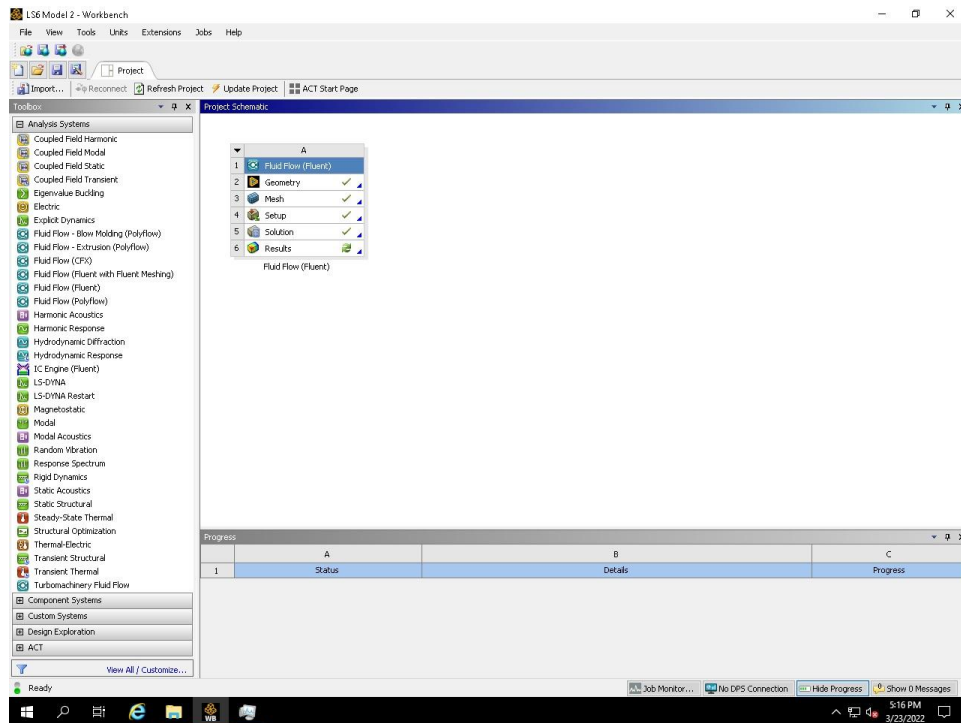

Figure X: ANSYS Workbench Main Interface

Any version of the manifold geometry could be used with ANSYS as long as the volume was continuous and contained no gaps. The runners and plenum of the manifolds were developed as separate part files and then joined together within Solidworks. This risked creating voids within the centers of each manifold, but we were creative in dimensioning the voids out of the manifolds. All manifold geometries were exported from Solidworks as a ".step" file so ANSYS SpaceClaim could read them. Figure X shows imported geometry within ANSYS SpaceClaim.

Here, the separate parts of the manifold were suppressed, allowing only the joined part to be read by ANSYS Meshing and Fluent.
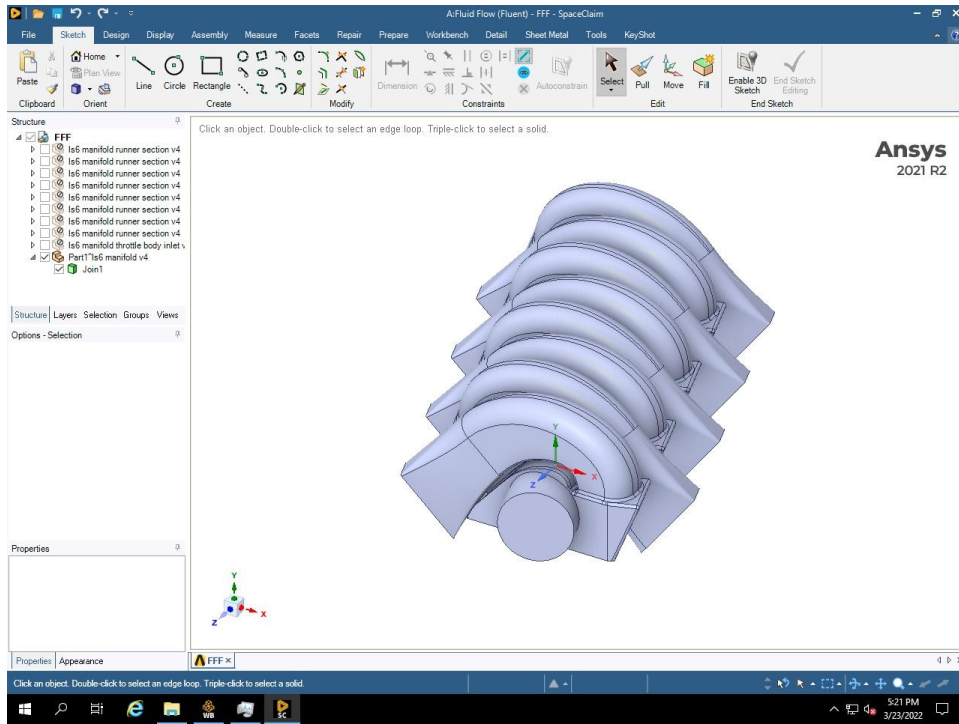

Figure X: Imported Geometry Inside ANSYS SpaceClaim

After geometry was imported into ANSYS, the next step was to define the mesh in ANSYS Meshing, shown in Figure X. The mesh is a discretization of the geometry that the solver can understand. Conceptually, it is the same as the control volume used to define the Navier-Stokes equations, but these cells are finite. For a given geometry, the number of cells is greater than one million, but this number generally depends on some meshing parameters. A larger number of cells means that the solution will be more accurate but it will take longer to converge. Additionally, the shapes of the cells impact the accuracy of the solution. Cells which are regular tend to create solutions which converge more quickly and accurately than those which are highly stretched. When the geometry of the part is not regular and includes sharp corners and tight spaces, the cells can become highly irregular. Tools within ANSYS Meshing can help alleviate these issues, but often the best solution is to simplify geometry where at all possible. This is why the solid models of the LS6 and Trailblazer SS manifolds could be simplified without risking the integrity of the solution. Quality tools inside ANSYS Meshing

show the maximum aspect ratio, orthogonality, skewness, element quality, and more of the current mesh. Additional parameters within this tool can be used to generate a higher quality mesh. ANSYS Fluent also contains tools to check the quality of the mesh. Most importantly, Fluent contains a tool that checks the minimum volume of all cells in the mesh. If the minimum value were less than or equal to zero, the mesh would be invalid and need to be regenerated. Meshing also is the stage in the process where inlets and outlets of the model are defined. They are defined at this stage because the mesh is generated using inflation. Inflation changes the size of the cells at the walls of the fluid volume. These simulations assumed that the velocity of the fluid at the walls is zero. But, the velocity changes very quickly from the wall to the freestream inside the manifolds. If the cells are large near the walls, the change is not captured correctly and the model is not accurate. By allowing inflation near the walls, the boundary layer is incorporated into the mesh. This matters for the inlet and outlets because inflation is not desired over the entire inlet and outlets, just at the walls. So by defining the inlet and outlets at this stage, the mesh can incorporate those openings and only generate inflated sections in the appropriate areas.
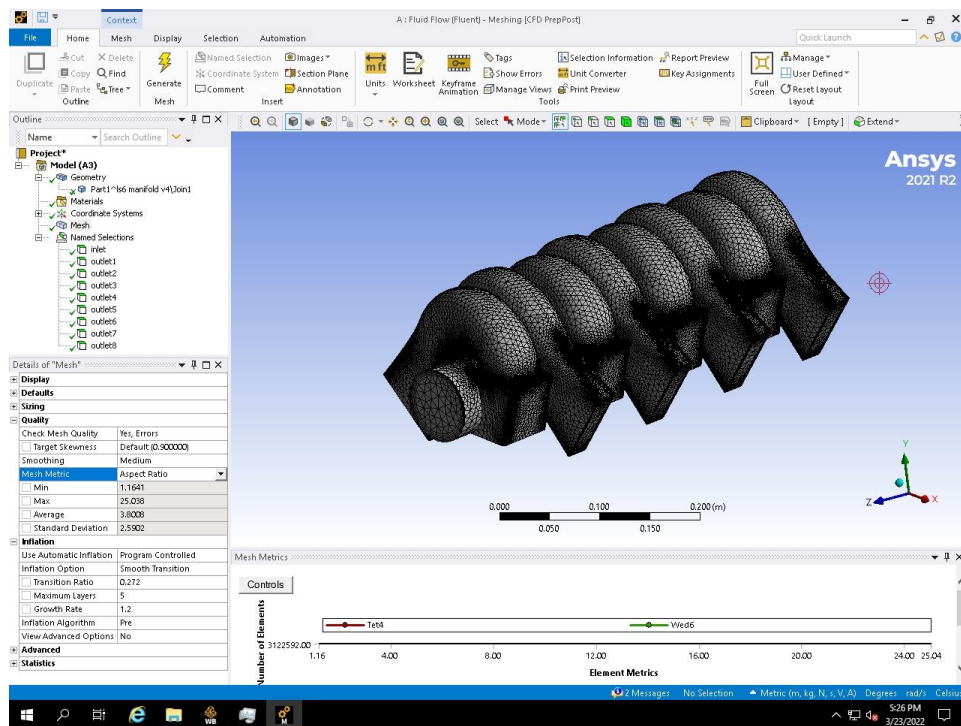

Figure X: ANSYS Meshing Interface with Options

After the geometry and mesh are defined within ANSYS, the Fluent solver can be used to create a model. Figure X shows the interface for Fluent. The solver uses the imported geometry and mesh with other parameters to generate a solution. This solution can be steady-state or transient. In either case, Fluent iterates the solver to try and balance the Navier-Stokes equations. The difference between the left and right-hand sides of these equations is captured in something called residuals. The residuals of a model tend to shrink with more iterations and good modeling parameters. Fluent defines convergence of a time-step in transient analysis or the solution in steady-state analysis as the iteration where the residuals fall below preset values. Ideally, the residuals of a converged solution would be zero, but due to round off errors usually the residuals of a model tend to some small value much less than 1. We monitored residuals in real-time during our simulations to make sure that our solutions converged. While residuals are not the only quality of a model to watch, they are a good first indication of convergence.
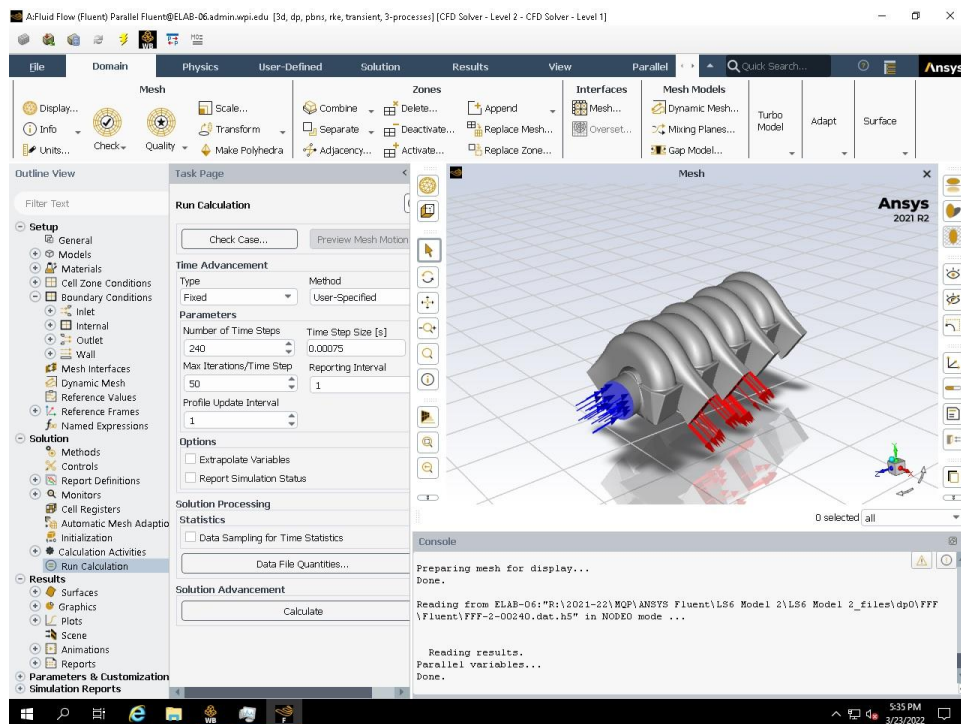

Figure X: ANSYS Fluent Interface

To model the opening and closing of the runners, the team utilized a script that would change the boundary conditions at the outlets of the manifold. We assumed that the engine speed was constant and that only two runners were open at any one time. In combination with the firing

order of the engine, we could define a pattern of open and closed runners. But, Fluent is not capable of defining a pattern to change boundary conditions on its own. So, we developed our own boundary condition changing script which would automatically change which runners were open at the appropriate time step according to the firing order and engine speed. This script was written in Scheme, a dialect of Lisp, and can be found in Appendix B.

The team defined the solid and fluid material properties of the manifold. Both manifolds only have air flowing through them. The air was defined as an ideal-gas with properties of specific heat, thermal conductivity, and viscosity defined as piecewise linear according to Table X in [heat transfer textbook]. The temperature range to take this data over was approximated using realistic values that were later confirmed by our initial data. For our simulations, that range was 250-400K. The solid material was only the wall of the manifold. The manifolds are both made from glass-fiber reinforced nylon. Fluent can use the Granta MDS materials database to select more exotic materials within a model. From that database, we chose to use nylon 6,6 containing 30-33% glass-fibers for our wall material.

We defined our initial boundary conditions for the model based on our initial data and a couple of assumptions. First, we assumed that the pressure inside the intake manifold is isobaric initially. Therefore, the MAP sensor reading could be used to directly define the gauge pressures at the inlets and outlets. Second, we assumed that the wall temperature was at some value larger than ambient. Thus, we added 20℉ to our ambient air temperature value taken from the IAT sensor. Third, we assumed that the backflow temperature from the outlets was at some value in between ambient and the coolant temperature. This value was defined as 162℉. Fourth, we assumed that the throttle is fully opened but the engine is not accelerating. This is not accurate to the real world. When a throttle is opened completely, the engine will continue to accelerate until it reaches its maximum speed. However, since the switching script cannot model that functionality, we are choosing to model constant speed with a fully opened throttle. Finally to simplify the pressure inputs, the operating pressure of the model was redefined as zero. By choosing this value, all the pressure values would be absolute pressure.

The team modeled the transient flow through each manifold for three four-stroke cycles. While only one full four-stroke cycle would be necessary for our analysis, the first cycle would contain garbage data as the model settled from the initial conditions. The energy equation for heat transfer between media was enabled. For the viscous model, the team chose to use the

realizable k-epsilon model. We chose this model on the advice of the ANSYS help documentation. The realizable k-epsilon model is useful for most types of fully turbulent flow. Only runners 1 and 3 were open at the start of the simulation, all other runners were modeled as walls. All solution methods were of the second-order variety for better accuracy. And lastly, the simulation was initialized from the inlet. Initializing the simulation is necessary to provide initial values for the solver to use. The inlet was chosen arbitrarily, all zones or an outlet could have also been chosen.

As few parameters as possible were modified within Fluent. There are hundreds of options inside Fluent that could change the way the solver creates the model. Thus, only the most important options were modified. The team summarized the parameters that were changed within ANSYS Meshing and Fluent to generate these models in Appendix C.

Analysis and Results

Dynamometer Testing

Baseline Data

Before beginning our work, to accurately analyze power gains as a direct result of optimized air flow through the engine, the group needed to gather preliminary data on the vehicle's performance. To achieve this, the vehicle was placed on a dynamometer to gather the horsepower and torque performance values of the engine. The specific dyno model used was a Dynocom 7500 Series with Eddy Current. This dynamometer uses a Frensia Eddy Current brake which allows the user to perform acceleration, step, sweep, and steady-state tests. The dyno is capable of testing torque values up to 7,500 ft-lbs and is rated for speeds up to 225 mph. The sensors for the roller speed take over 100 samples/rpm, compared to other dynos which typically only read 20-60 samples/rpm. The timing accuracy of the dyno reads within +/- 0.1 μs. The drum speed readings are accurate to +/- 0.001 mph and the revolutions per minute engine readings are accurate to +/- 0.01 rpm. The increased sensitivity provides the user with the most detailed and accurate information possible. The Dynocom 7500 Series is also capable of simulating a ¼ mile drag strip or circle track laps, but this feature will not be needed for our testing as our Corvette will be driven mostly on the street.
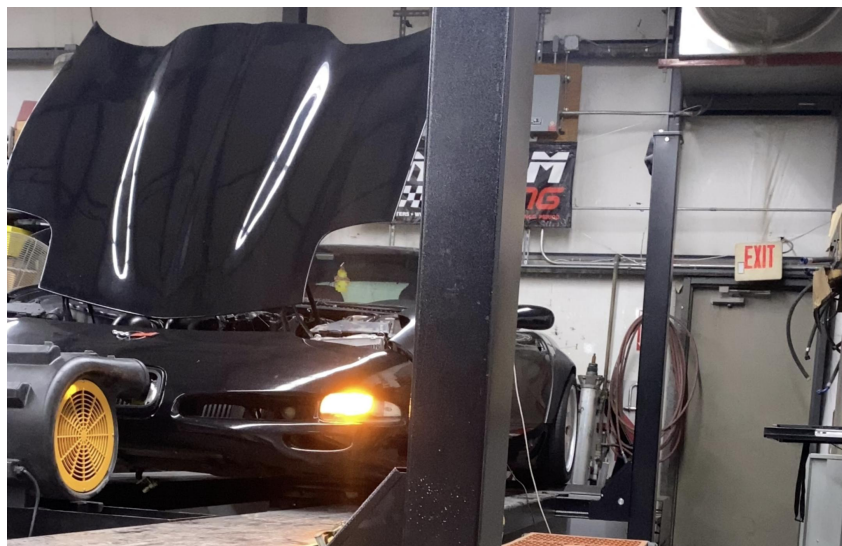
Figure X: Corvette Ready & Secured on the Dynamometer

The group was able to put the vehicle on the dyno very early on in the project with the help of Paul Thompson. This allowed us to accurately judge the car's current engine airflow state in terms of the horsepower and torque values generated, and also provided us the opportunity to address any existing performance issues the vehicle may have had before our work began. In the run the vehicle had on the dynamometer, the graphs displayed 337 horsepower and 347 foot-pounds of torque being generated, which includes the minor losses through the vehicle's drivetrain. All numbers taken from the dyno used in our data account for drivetrain losses, as the dyno we had access to measures torque produced at the wheels rather than at the flywheel. Below you can reference the chart following the dyno run as well as the vehicle placed on the dynamometer.
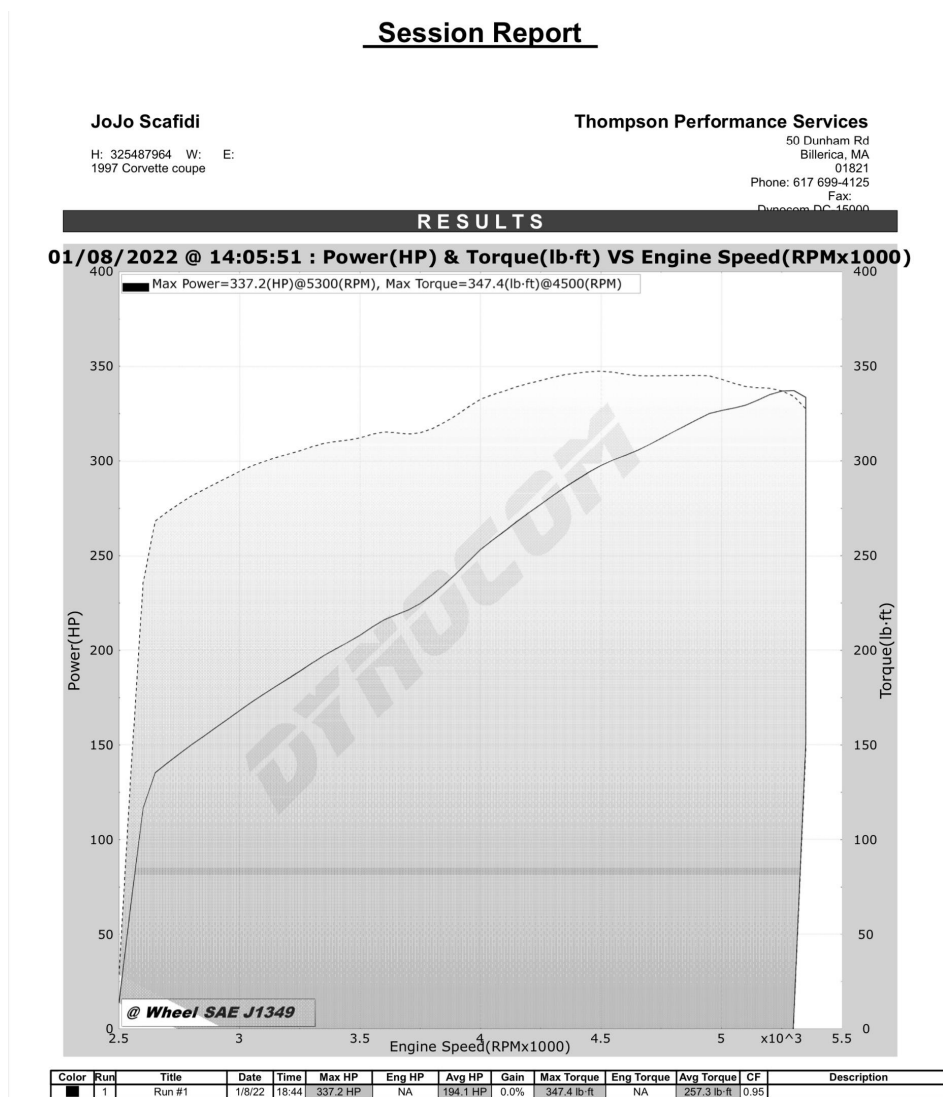

Figure X: Preliminary Horsepower & Torque Value Graphs

Final Data

Engine Swap, 241 Heads, Jam Cam, LS6 Intake Manifold, Restrictor Plate, Fuel Pump, and Methanol

Engine Swap, 241 Heads, Jam Cam, LS6 Intake Manifold, Restrictor Plate Removed, Fuel Pump, and Methanol

Engine Swap, 799 Heads, Jam Cam, LS6 Intake Manifold, Restrictor Plate Removed, Fuel Pump, and Methanol

Engine Swap, 799 Heads, Jam Cam, Trailblazer Intake Manifold, Restrictor Plate Removed, Fuel Pump, and Methanol

Intake Manifold Flow Simulation Results

The original purpose of our simulations were to determine if we could model airflow through our intake system to predict power development. We scaled this goal back to modeling the differences between each intake manifold. A manifold performs well if it can move air with little resistance. The manifold is designed by the manufacturer in such a way to facilitate filling the cylinders with air quickly. If more air can flow into a cylinder for a given engine speed, more power can be developed at the wheels of the car. So, a manifold that can flow more air should help an engine develop more power. This is not the only consideration related to manifold geometry for power, but it will be the one that this analysis tests.

Our initial simulations utilized a simpler prototype manifold geometry to test the simulation parameters. The benefit of a simpler initial geometry is that simulations finish within a couple of hours rather than six, ten, or twenty-four hours. This means that different parameters can be tested and changed on geometry that has some similarities to the final models. The results on the simple geometry were not accurate, but it provided a nice test bed to check expected results and trial different graphics so that the simulations on the complex geometry could be run once.

Airflow within the LS6 and Trailblazer SS intake manifolds was simulated in ANSYS Fluent. Table X summarizes the initial boundary conditions of the simulations as well as the duration of the model. Effectively, the environment that the team tried to recreate in Fluent was one where the engine was operating at a constant 2000 RPM at wide-open throttle. Parameters for temperature, flow, and pressure were taken from our initial dynamometer data with the LS1 engine and the LS6 intake manifold. These conditions were then applied to both the LS6 and the Trailblazer SS manifolds. Therefore, engine speed and mass airflow were held constant between each manifold. The difference in flow at the outlets were measured and recorded by ANSYS for each time step. The manifold that flowed the most volume air for these conditions would be the better performing manifold according to simulation.

Physical Parameter	Value
Intake Air Temperature	75 ℉
Manifold Absolute Pressure (Isobaric)	43.3 kPa$_a$
Intake Mass Airflow	4.13 lbm/min
Wall Temperature	95 ℉
Outlet Backflow Temperature	162 ℉
Engine Speed	2000 RPM
Total Simulation Run Time	0.18 s

Table X: Simulation Initial Boundary Conditions

Fluent monitored the volumetric flow rate at the outlets of the runners for each time step. To calculate the total volume of air moved, the integral of the volumetric flow rate was taken with respect to time. The result was the amount of air moved in cubic feet by each runner. The simulation modeled three four-stroke cycles, but the data for the first of those cycles was muddied by the solver. Therefore, only the second and third cycles can be considered. Table X shows the volume of air flowed by each open runner, the inlet, and the total volume flowed for the LS6 manifold. Table X shows the same kind of data for the Trailblazer SS manifold. Appendix D contains the raw data used to summarize the flow data shown below. Appendix E contains all of the flow vs. time plots for each manifold.

Inlet/Outlet	Volume in Cycle #2 [ft^3]	Volume in Cycle #3 [ft^3]	Total Volume Flowed [ft^3]
Throttle			
Runner #1			
Runner #2			
Runner #3			
Runner #4			
Runner #5			
Runner #6			
Runner #7			
Runner #8			
Total Air Out			
Delta?			

Table X: LS6 Manifold Flow Data

Inlet/Outlet	Volume in Cycle #2 [ft³]	Volume in Cycle #3 [ft³]	Total Volume Flowed [ft³]
Throttle			
Runner #1			
Runner #2			
Runner #3			
Runner #4			
Runner #5			
Runner #6			
Runner #7			
Runner #8			
Total Air Out			
Delta?			

Table X: Trailblazer SS Manifold Flow Data

The plots of volumetric flow vs. time for the runners all have a similar shape. Figure X shows a typical plot for volumetric flow over time at the outlet of a runner. Flow rate increases the longer the runner is open. This conclusion is valid from a physical perspective because it takes time for the air to accelerate through the runner. While the runner is closed, air is not moving inside it. When the runner opens, air is drawn through the runner from the plenum as the piston pulls air into the cylinder. This is modeled as a source of mass flow into the manifold. The velocity of the air continues to increase as open runner duration increases because the pressure gradient between inlet and outlet is changing. Figures X-X show the pressure gradient on the middle plane of the manifold as well as a plane intersecting runner #6 over four time steps. As time increases, the gradient between inlet and outlet also increases.

Figure X: Volumetric Flow vs. Time for Runner #6 of LS6 Manifold

d	

Figure X: Pressure Plot of LS6 Manifold Through Plenum Cross-Section and Runner #6
Cross-Section at Four Time Steps

According to the data in <mark>Tables</mark> X and X, the manifold which flows more air for a given runner open time and mass air flow is the _____ manifold. This makes sense since the _____ manifold has _____ runners and a _____ plenum. One limitation of this conclusion is that the mass flow rates at the inlet are both constant, but the opening for the throttles are different. This means that the cross-sectional areas of the openings are different. Assuming a constant density between models, to maintain equivalent mass flow rates the velocity of air moving into the Trailblazer SS manifold must decrease compared to the LS6 manifold. The effects of this are apparent in <mark>Figures</mark> X-X. For the same instant in time, the velocity through the plenums and exits of the runners are ___ for the Trailblazer SS manifold compared to the LS6 manifold.

d	

Figure X: Velocity Through the Plenums (Top) and Runner #6 Exits (Bottom) of LS6 Manifold (Left) and Trailblazer SS Manifold (Right)

An interesting observation of the data is that mass flow through the manifold is not net-zero at all instances in time. Figures X and X show the net mass flow through the LS6 and Trailblazer SS manifolds, respectively, over the duration of the simulation. These figures illustrate why roughly the first half of the first four-stroke cycle contains useless data: the mass flow through the manifold has not stabilized enough from the initial conditions. The fluctuation of the net mass flow rate does not tend to zero after that period, though. It continues to fluctuate between ____ and ____. According to the flow rate plots Figures E1-E9 and E11-E19 in Appendix E, there is still flow into the inlet and out of the runners during the fluctuations for both manifolds, implying that the flow does not reverse. This implies that the nonzero net mass flow rate is being caused by pressure fluctuations in the manifold occurring on a short time scale. If the switching aspect of the model were ignored and the manifold were allowed to enter steady-state flow through just two runners, most likely the net mass flow quantity would tend to zero as pressure fluctuations settled down. Taking the integral of the second and third four-stroke cycles shows that the net change in mass inside either manifold is ____.

Figure X: Net Mass Flow in LS6 Manifold

Figure X: Net Mass Flow in Trailblazer SS Manifold

At the time of writing, the dynamometer tests of the new engine have not been completed. Therefore, our conclusion that the ＿＿＿ manifold produces more power because it flows more air cannot yet be verified.

Conclusions and Areas for Further Improvement

The group saw tremendous success not only in the improvement and optimization of air flow through the engine, but also managing numerous moving parts and avoiding any problems upon the reassembly of the engine and vehicle. Many modifications, performance parts and equipment were utilized in improving the flow of air through the engine and supporting the increased forces that resulted from the higher power output.

8 rib belt

8 nozzle meth injection

Aftermarket intake manifold

Aftermarket heads - porting

Upgraded pulley

Upgraded blower

Lightweight flywheel

Larger diameter header runners

Throttle body

Bibliography

Appendix A

Simplified Geometry Models
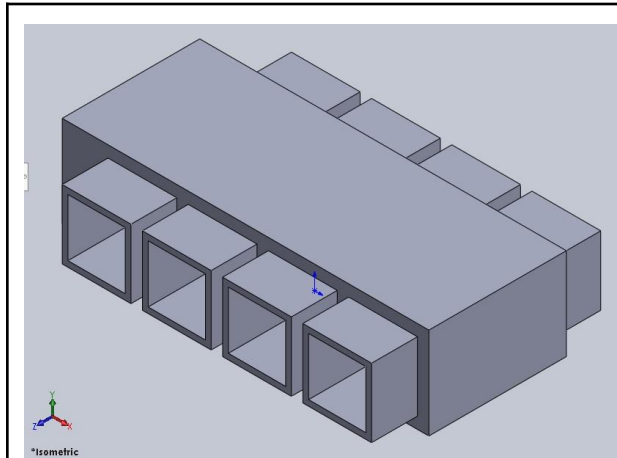
Figure A1: First Prototype Isometric View
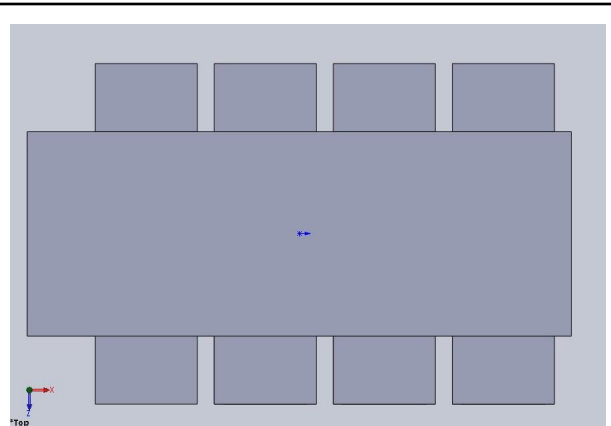
Figure A2: First Prototype Top View
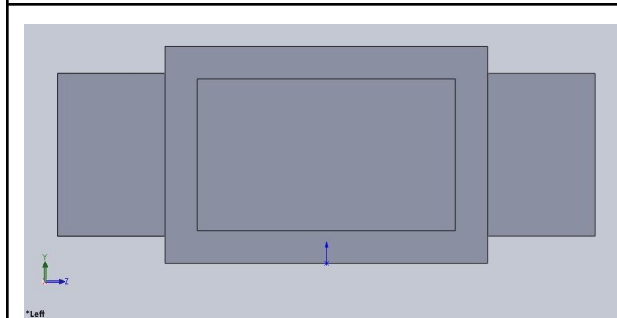
Figure A3: First Prototype Front View
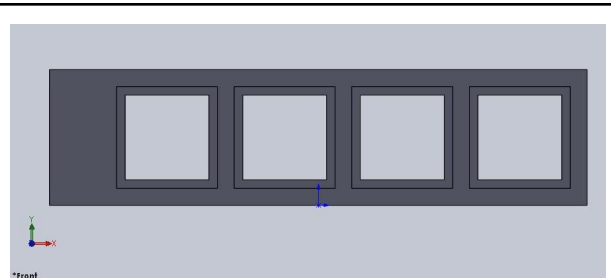
Figure A4: First Prototype Side View
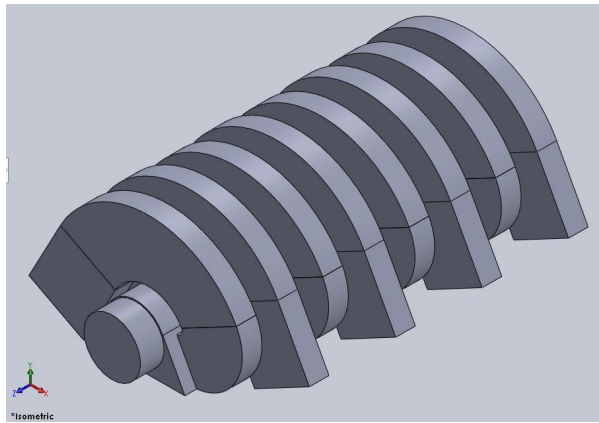
Figure A5: Second Prototype Isometric View
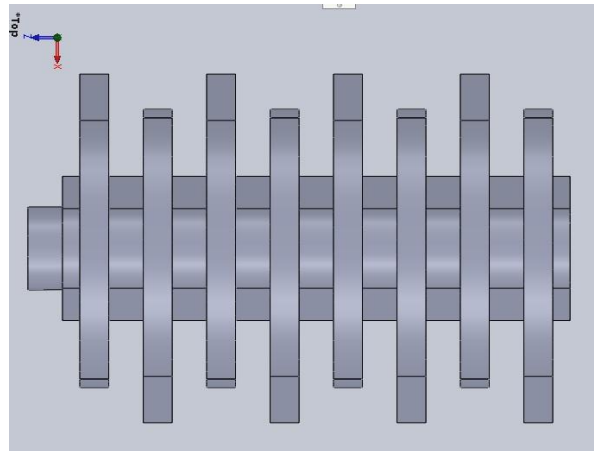

Figure A6: Second Prototype Top View
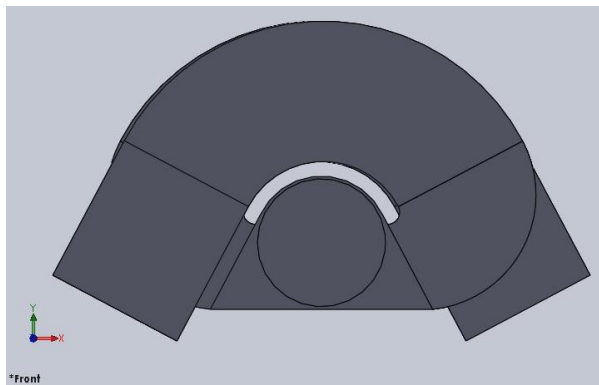
Figure A7: Second Prototype Front View
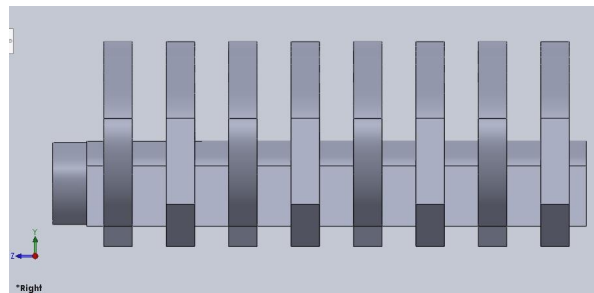
Figure A8: Second Prototype Side View

LS6 Models
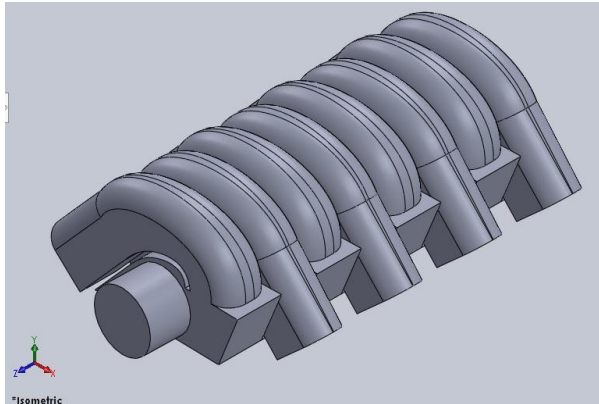
Figure A9: LS6 Mark 1 Isometric View
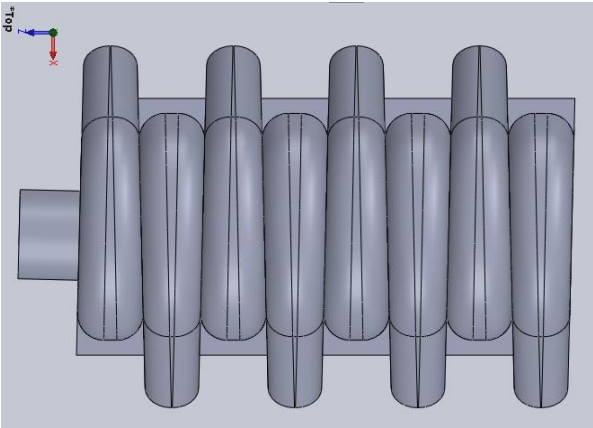

Figure A10: LS6 Mark 1 Top View
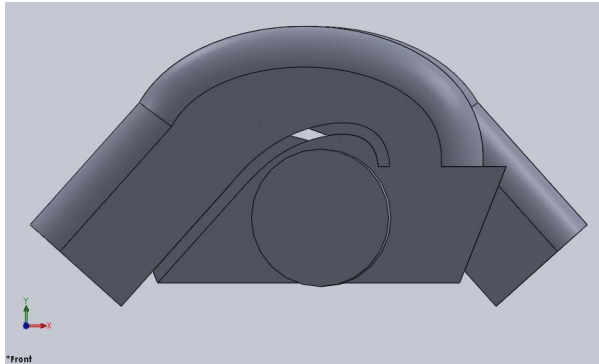
Figure A11: LS6 Mark 1 Front View
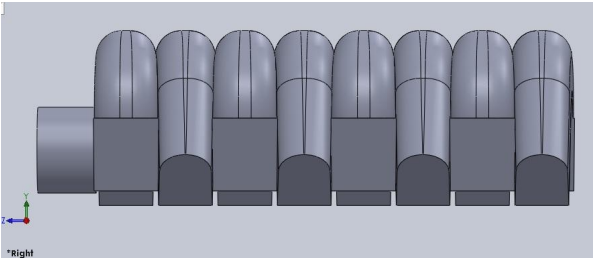

Figure A12: LS6 Mark 1 Side View
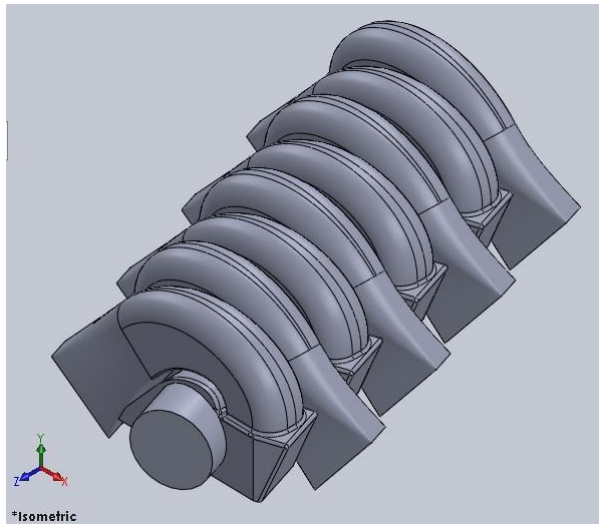
Figure A13: LS6 Mark 2 Isometric View
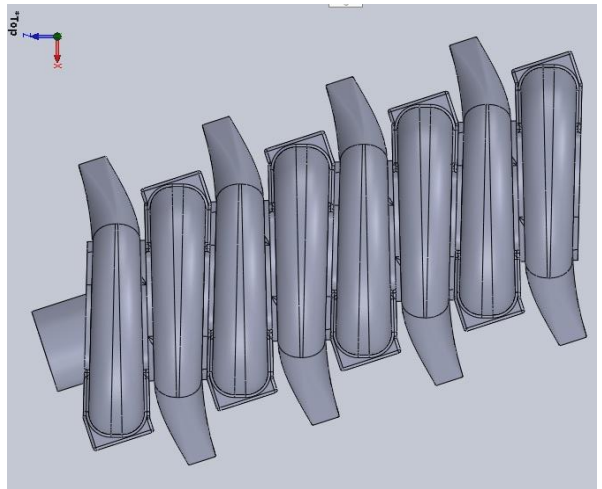
Figure A14: LS6 Mark 2 Top View
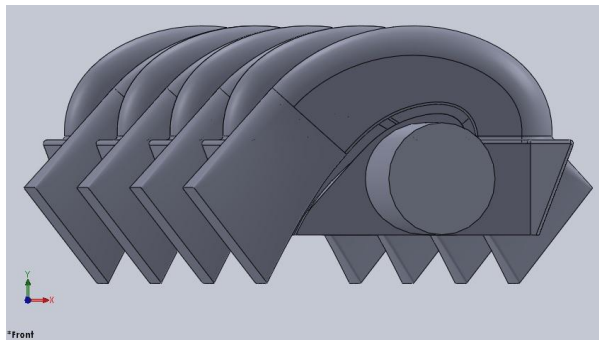
Figure A15: LS6 Mark 2 Front View
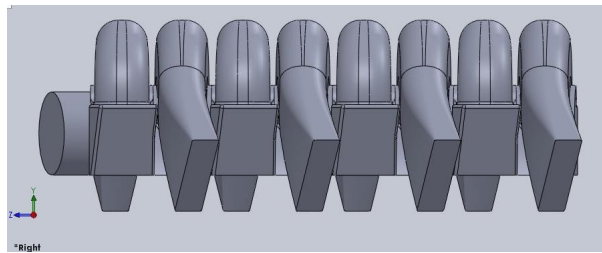
Figure A16: LS6 Mark 2 Side View

Trailblazer SS Models
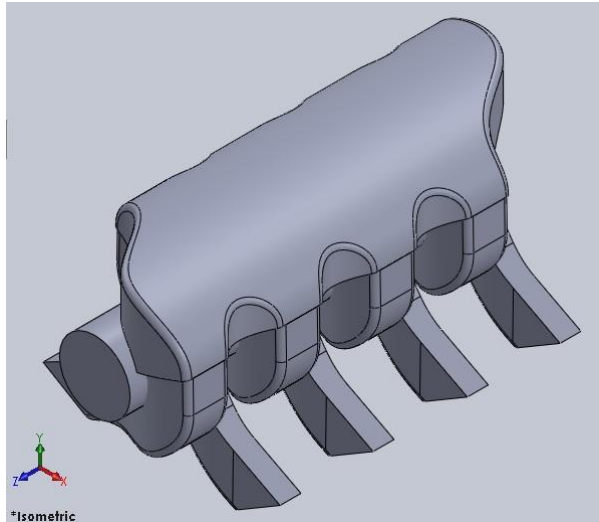
Figure A17: Trailblazer SS Mark 1 Isometric View
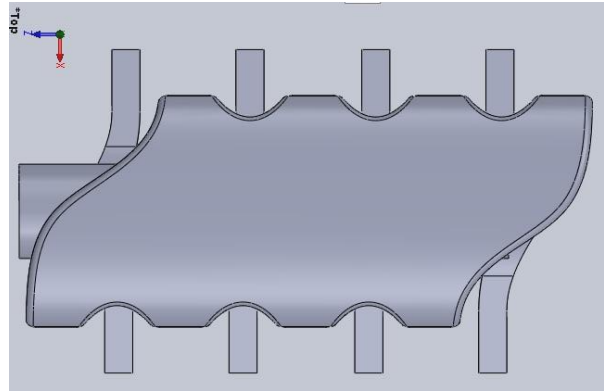
Figure A18: Trailblazer SS Mark 1 Top View
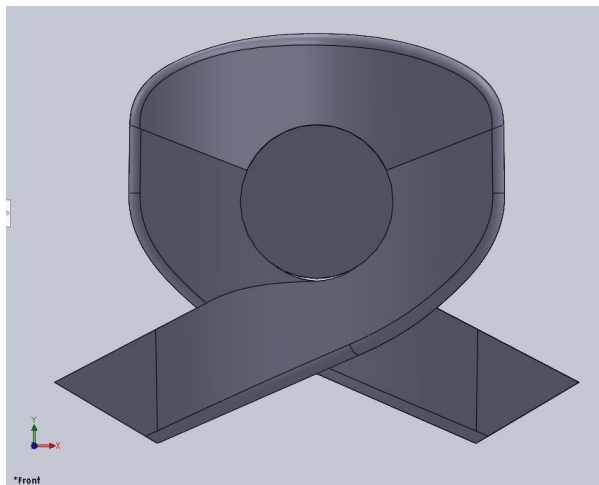
Figure A19: Trailblazer SS Mark 1 Front View
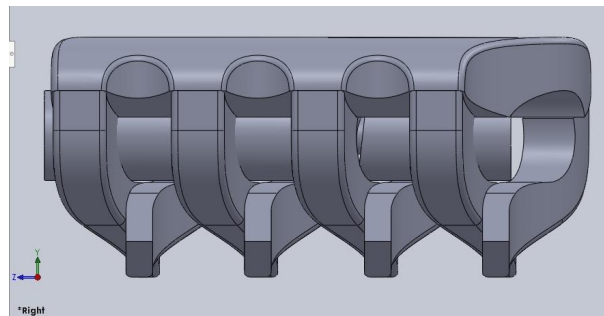
Figure A20: Trailblazer SS Mark 1 Side View
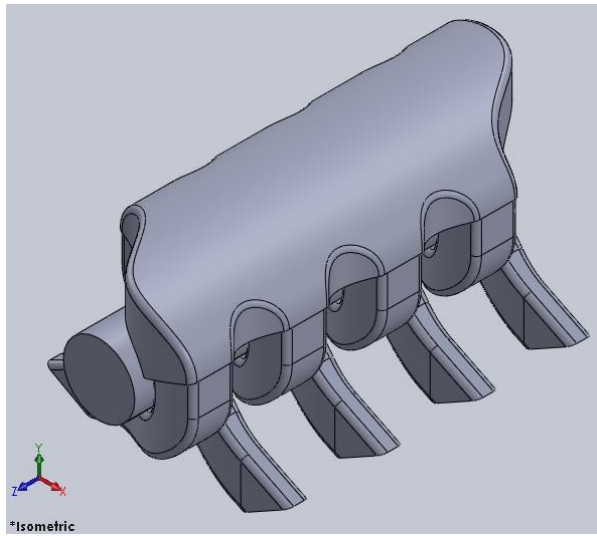
Figure A21: Trailblazer SS Mark 2 Isometric
View
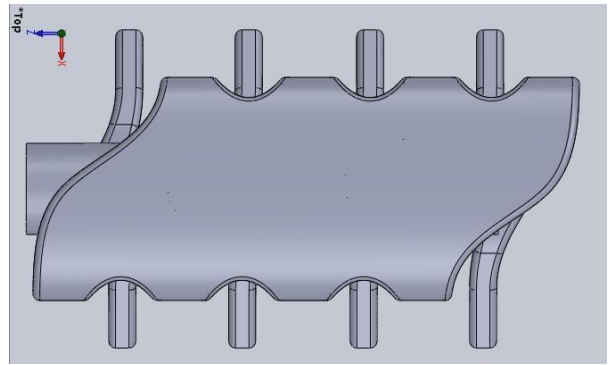

Figure A22: Trailblazer SS Mark 2 Top View
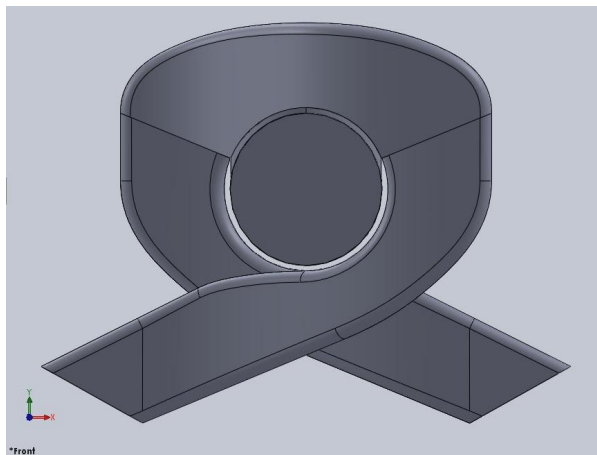
Figure A23: Trailblazer SS Mark 2 Front
View
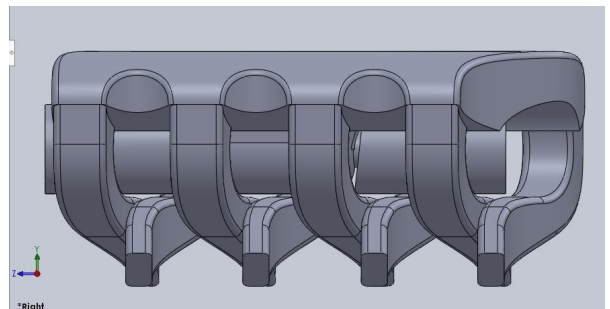
Figure A24: Trailblazer SS Mark 2 Side View

Appendix B

```scheme
1  (define (changeboundary)
2
3  ;; unused
4  (define timespan (%rpgetvar 'flow-time))
5  (define deltat (%rpgetvar 'physical-time-step))
6  ;; constants
7  (define nettime (%rpgetvar 'number-of-time-steps))
8  (define ncycle 3)
9  (define nstate 8)
10 (define period (/ nettime ncycle))
11 (define switch (/ nettime (* ncycle nstate)))
12 ;; variable terms
13 (define counter (%rpgetvar 'time-step))
14 (define cswitch (remainder counter switch))
15 (define revolv (floor(/ counter period)))
16 (define flag (- counter (* period revolv)))
17 ;; print debug
18 (newline)
19 (display "time spanned [s]: ")(display timespan)(newline)
20 (display "time step size [s]: ")(display deltat)(newline)
21 (display "number of time steps: ")(display nettime)(newline)
22 (display "number of cycles: ")(display ncycle)(newline)
23 (display "number of outlet states: ")(display nstate)(newline)
24 (display "period length [time step]: ")(display period)(newline)
25 (display "switch every 'n' time steps: ")(display switch)(newline)
26 (display "current time step: ")(display counter)(newline)
27 (display "switching counter: ")(display cswitch)(newline)
28 (display "period counter: ")(display revolv)(newline)
29 (display "state counter: ")(display flag)(newline)
30
31 ;; outlet switching algorithm
32 (cond
33    ((= cswitch 0) (display "switch outlets")(newline)
34    (cond
35       ((= flag (* 0 switch))
36          (display "4th closes 1st opens")(newline)
37          (ti-menu-load-string "/define/boundary-conditions/zone-type outlet4 wall")
38          (ti-menu-load-string "/define/boundary-conditions/wall outlet4 0 no 0 no yes
             temperature no 95 no no no no 0 no 0.5 no 1")
39          (ti-menu-load-string "/define/boundary-conditions/zone-type outlet1 pressure-
             outlet")
40          (ti-menu-load-string "/define/boundary-conditions/pressure-outlet outlet1 yes no
             43300 no 162 no yes no no yes 5 10 yes yes no no no")
```

Figure B1: changeboundary.scm Lines 1-40

```
40              (ti-menu-load-string "/define/boundary-conditions/pressure-outlet outlet1 yes no
                43300 no 162 no yes no no yes 5 10 yes yes no no no")
41          )
42      ((= flag (* 1 switch))
43          (display "3rd closes 8th opens")(newline)
44          (ti-menu-load-string "/define/boundary-conditions/zone-type outlet3 wall")
45          (ti-menu-load-string "/define/boundary-conditions/wall outlet3 0 no 0 no yes
                temperature no 95 no no no no 0 no 0.5 no 1")
46          (ti-menu-load-string "/define/boundary-conditions/zone-type outlet8 pressure-
                outlet")
47          (ti-menu-load-string "/define/boundary-conditions/pressure-outlet outlet8 yes no
                43300 no 162 no yes no no yes 5 10 yes yes no no no")
48          )
49      ((= flag (* 2 switch))
50          (display "1st closes 7th opens")(newline)
51          (ti-menu-load-string "/define/boundary-conditions/zone-type outlet1 wall")
52          (ti-menu-load-string "/define/boundary-conditions/wall outlet1 0 no 0 no yes
                temperature no 95 no no no no 0 no 0.5 no 1")
53          (ti-menu-load-string "/define/boundary-conditions/zone-type outlet7 pressure-
                outlet")
54          (ti-menu-load-string "/define/boundary-conditions/pressure-outlet outlet7 yes no
                43300 no 162 no yes no no yes 5 10 yes yes no no no")
55          )
56      ((= flag (* 3 switch))
57          (display "8th closes 2nd opens")(newline)
58          (ti-menu-load-string "/define/boundary-conditions/zone-type outlet8 wall")
59          (ti-menu-load-string "/define/boundary-conditions/wall outlet8 0 no 0 no yes
                temperature no 95 no no no no 0 no 0.5 no 1")
60          (ti-menu-load-string "/define/boundary-conditions/zone-type outlet2 pressure-
                outlet")
61          (ti-menu-load-string "/define/boundary-conditions/pressure-outlet outlet2 yes no
                43300 no 162 no yes no no yes 5 10 yes yes no no no")
62          )
63      ((= flag (* 4 switch))
64          (display "7th closes 6th opens")(newline)
65          (ti-menu-load-string "/define/boundary-conditions/zone-type outlet7 wall")
66          (ti-menu-load-string "/define/boundary-conditions/wall outlet7 0 no 0 no yes
                temperature no 95 no no no no 0 no 0.5 no 1")
67          (ti-menu-load-string "/define/boundary-conditions/zone-type outlet6 pressure-
                outlet")
68          (ti-menu-load-string "/define/boundary-conditions/pressure-outlet outlet6 yes no
                43300 no 162 no yes no no yes 5 10 yes yes no no no")
```

Figure B2: changeboundary.scm Lines 40-68

```
66        »       »       »     (ti-menu-load-string "/define/boundary-conditions/wall outlet7 0 no 0 no yes
   ↵                              temperature no 95 no no no no 0 no 0.5 no 1")
67        »       »       »     (ti-menu-load-string "/define/boundary-conditions/zone-type outlet6 pressure-
   ↵                              outlet")
68        »       »       »     (ti-menu-load-string "/define/boundary-conditions/pressure-outlet outlet6 yes no
   ↵                              43300 no 162 no yes no no yes 5 10 yes yes no no no")
69        »       »       )
70        »       »       ((= flag (* 5 switch))
71        »       »       »     (display "2nd closes 5th opens")(newline)
72        »       »       »     (ti-menu-load-string "/define/boundary-conditions/zone-type outlet2 wall")
73        »       »       »     (ti-menu-load-string "/define/boundary-conditions/wall outlet2 0 no 0 no yes
   ↵                              temperature no 95 no no no no 0 no 0.5 no 1")
74        »       »       »     (ti-menu-load-string "/define/boundary-conditions/zone-type outlet5 pressure-
   ↵                              outlet")
75        »       »       »     (ti-menu-load-string "/define/boundary-conditions/pressure-outlet outlet5 yes no
   ↵                              43300 no 162 no yes no no yes 5 10 yes yes no no no")
76        »       »       )
77        »       »       ((= flag (* 6 switch))
78        »       »       »     (display "6th closes 4th opens")(newline)
79        »       »       »     (ti-menu-load-string "/define/boundary-conditions/zone-type outlet6 wall")
80        »       »       »     (ti-menu-load-string "/define/boundary-conditions/wall outlet6 0 no 0 no yes
   ↵                              temperature no 95 no no no no 0 no 0.5 no 1")
81        »       »       »     (ti-menu-load-string "/define/boundary-conditions/zone-type outlet4 pressure-
   ↵                              outlet")
82        »       »       »     (ti-menu-load-string "/define/boundary-conditions/pressure-outlet outlet4 yes no
   ↵                              43300 no 162 no yes no no yes 5 10 yes yes no no no")
83        »       »       )
84        »       »       ((= flag (* 7 switch))
85        »       »       »     (display "5th closes 3rd opens")(newline)
86        »       »       »     (ti-menu-load-string "/define/boundary-conditions/zone-type outlet5 wall")
87        »       »       »     (ti-menu-load-string "/define/boundary-conditions/wall outlet5 0 no 0 no yes
   ↵                              temperature no 95 no no no no 0 no 0.5 no 1")
88        »       »       »     (ti-menu-load-string "/define/boundary-conditions/zone-type outlet3 pressure-
   ↵                              outlet")
89        »       »       »     (ti-menu-load-string "/define/boundary-conditions/pressure-outlet outlet3 yes no
   ↵                              43300 no 162 no yes no no yes 5 10 yes yes no no no")
90        »       »       )
91        »       ))
92        »       (else (display "maintain outlets")(newline))
93  )
94
95  )
96
```

Figure B3: changeboundary.scm Lines 66-96

Appendix C

Menu Path	Value
SpaceClaim/Non-Joined Part/Check Box	Deselect box, right-click and deactivate for physics
Meshing/Mesh/Defaults/Element Size	1.0e-2 m
Meshing/Mesh/Inflation/Use Automatic Inflation	Program Controlled
Fluent/Setup/General/Units/Mass Flow	lbm/min
Fluent/Setup/General/Units/Temperature	F
Fluent/Setup/General/Mesh/Units/Volume-Flow-Rate	ft^3/s
Fluent/Setup/General/Mesh/Check	Minimum volume greater than zero
Fluent/Setup/General/Mesh/Report Quality	Maximum aspect ratio less than 3.5e1, minimum orthogonal quality greater than 1e-1
Fluent/Setup/General/Solver/Time	Transient
Fluent/Setup/Models/Energy	On
Fluent/Setup/Models/Viscous	K-epsilon, realizable
Fluent/Setup/Materials/Fluid/Air/Density	ideal-gas
Fluent/Setup/Materials/Fluid/Air/Specific Heat	Piecewise, use 250-400K values in heat transfer textbook

Fluent/Setup/Materials/Fluid/Air/Thermal Conductivity	Piecewise, use 250-400K values in heat transfer textbook
Fluent/Setup/Materials/Fluid/Air/Viscosity	Piecewise, use 250-400K values in heat transfer textbook
Fluent/Setup/Materials/Solid/Right-Click/New	Granta MDS Database, plastic-pa66-30-33%-glass-fiber, Copy
Fluent/Setup/Boundary Conditions/Inlet/Type	mass-flow-inlet
Fluent/Setup/Boundary Conditions/Inlet/Momentum	mass flow=4.13, supersonic gauge pressure=43300, direction=normal to boundary
Fluent/Setup/Boundary Conditions/Inlet/Thermal	total temperature=75
Fluent/Setup/Boundary Conditions/Outlet/Momentum	gauge pressure=43300
Fluent/Setup/Boundary Conditions/Outlet/Thermal	backflow total temperature=162
Fluent/Setup/Boundary Conditions/Wall/Thermal/Thermal Conditions/Temperature	temperature=95
Fluent/Setup/Boundary Conditions	outlet1 & outlet 3 pressure-outlet only
Fluent/Setup/Boundary Conditions/Operating Conditions/Operating Pressure	0
Fluent/Solution/Methods/Spatial Discretization/Turbulent Kinetic Energy	Second Order Upwind

Fluent/Solution/Methods/Spatial Discretization/Turbulent Dissipation Rate	Second Order Upwind
Fluent/Solution/Report Definitions/Right Click/New/Surface Report/Volume Flow Rate	One for each inlet and outlet, change name and pick corresponding surface
Fluent/Solution/Report Definitions/Right Click/New/	Select all inlets and outlets, rename to 'net-mflow'
Fluent/Solution/Monitors/Convergence Conditions/Right Click/Create	Click add, then pick report definition as 'net-mflow' with stop criterion 0.001
Fluent/Solution/Initialization/Compute from	inlet
Fluent/Solution/Calculation Activities/Execute Commands	/file/read-macros "R:\2021-22\MQP\ANSYS Fluent\<model name>\changeboundary.scm" (changeboundary)
Fluent/Solution/Calculation Activities/Execute Commands/When	Every 1 Time Step
Fluent/Solution/Run Calculation/Number of Time Steps	240
Fluent/Solution/Run Calculation/Time Step Size	0.00075
Fluent/Solution/Run Calculation/Max Iterations per Time Step	50
Fluent/Results/Surfaces/New	Plane in ZX called midplane (pick distance per manifold)
Fluent/Results/Surfaces/New	Plane in XY called runner5plane (pick distance per manifold)

Fluent/Results/Graphics/Contours/New	\<plane\>-pressure in total pressure with contour lines
Fluent/Results/Graphics/Contours/New	\<plane\>-velocity in velocity magnitude with contour lines
Fluent/Results/Graphics/Contours/New	\<plane\>-temperature in total temperature with contour lines
Fluent/Results/Graphics/Contours/New	\<plane\>-density in density magnitude with contour lines
Fluent/Solution/Calculation Activities/Solution Animations/New	\<contour\>-animation every 1 time step

https://images.app.goo.gl/rdTMBcGv1eqNx7pT6

Appendix D

Table D1: Volumetric Flow Data for LS6 Manifold

Table D2: Volumetric Flow Data for Trailblazer SS Manifold

Appendix E

Figure E1: Volumetric Flow vs. Time of LS6 Manifold Inlet

Figure E2: Volumetric Flow vs. Time of LS6 Manifold Outlet #1

Figure E3: Volumetric Flow vs. Time of LS6 Manifold Outlet #2

Figure E4: Volumetric Flow vs. Time of LS6 Manifold Outlet #3

Figure E5: Volumetric Flow vs. Time of LS6 Manifold Outlet #4

Figure E6: Volumetric Flow vs. Time of LS6 Manifold Outlet #5

Figure E7: Volumetric Flow vs. Time of LS6 Manifold Outlet #6

Figure E8: Volumetric Flow vs. Time of LS6 Manifold Outlet #7

Figure E9: Volumetric Flow vs. Time of LS6 Manifold Outlet #8

Figure E10: Net Mass Flow vs. Time of LS6 Manifold

Figure E11: Volumetric Flow vs. Time of Trailblazer SS Manifold Inlet

Figure E12: Volumetric Flow vs. Time of Trailblazer SS Manifold Outlet #1

Figure E13: Volumetric Flow vs. Time of Trailblazer SS Manifold Outlet #2

Figure E14: Volumetric Flow vs. Time of Trailblazer SS Manifold Outlet #3

Figure E15: Volumetric Flow vs. Time of Trailblazer SS Manifold Outlet #4

Figure E16: Volumetric Flow vs. Time of Trailblazer SS Manifold Outlet #5

Figure E17: Volumetric Flow vs. Time of Trailblazer SS Manifold Outlet #6

Figure E18: Volumetric Flow vs. Time of Trailblazer SS Manifold Outlet #7

Figure E19: Volumetric Flow vs. Time of Trailblazer SS Manifold Outlet #8

Figure E20: Net Mass Flow vs. Time of Trailblazer SS Manifold